UNIVERSITÉ DE MONTRÉAL

INVERSE HEAT CONDUCTION PROBLEM WITH A MOVING BOUNDARY

XIN LIU
DÉPARTEMENT DE GÉNIE MÉCANIQUE
ÉCOLE POLYTECHNIQUE DE MONTRÉAL

MÉMOIRE PRÉSENTÉ EN VUE DE L'OBTENTION
DU DIPLÔME DE MAÎTRISE ÈS SCIENCES APPLIQUÉES
(GÉNIE MÉCANIQUE)
JUIN 2002

© Xin Liu, 2002.

UNIVERSITÉ DE MONTRÉAL

ÉCOLE POLYTECHNIQUE DE MONTRÉAL

Ce mémoire intitulé :

INVERSE HEAT CONDUCTION PROBLEM
WITH A MOVING BOUNDARY

présenté par : LIU Xin
en vue de l'obtention du diplôme de : Maîtrise ès sciences appliquées
a été dûment accepté par le jury d'examen constitué de :

M. VASSEUR Patrick, Ph.D., président
M. PRUD'HOMME Michel, Ph.D., membre et directeur de recherche
M. NGUYEN The Hung, Ph.D., membre et codirecteur de recherche
M. ROBILLARD Luc, D.Sc., membre

Dedicated to my wife, my son and my parents

ACKNOWLEDGEMENT

I would like to express my greatest appreciation to my director, Professor Michel Prud'homme, not only for his patience, rigor in examining all the mathematical formula in this thesis, but also for his encouragement and friendly guidance during the course of this thesis. I am very pleased to have the opportunity to work under his supervision and counseling in all phases of my graduate study at Ecole Polytechnique, University of Montreal.

I am also deeply indebted to Professor T. Hung Nguyen, my co-director, for not only giving me the opportunity to work on so exciting project but also his wise guidance and continuous support. I consider it a great pleasure to study and work under his supervision and consultant. I have benefited from many enlighting discussions with him. He is always patient and encouraging.

Grateful acknowledgements are also expressed to Hui Jiang and my other fellow graduate students and colleagues in Department of Mechanical Engineering for many invaluable discussions both in professional and in computer knowledge.

Thanks are given to my wife Jun Yu for her love, encouragement, support and also for her many useful suggestions during my graduate study.

Finally, I would like to sincerely thank to my thesis defense jury for their examination of my thesis.

RÉSUMÉ

L'objectif de ce mémoire est d'introduire une méthode qui sert à résoudre le problème inverse de conduction de chaleur en utilisant une frontière mobile et en ayant recours à la méthode du gradient conjugué et des équations adjointes. Cette approche requiert la dérivation de trois équations, soit l'équation directe, l'équation de sensibilité et l'équation adjointe.

Dans l'introduction, ce travail fait l'exposé d'études existantes sur le problème direct ainsi que sur le problème inverse de conduction de chaleur. Le premier chapitre présente la dérivation des équations gouvernantes sans dimension.

Le deuxième chapitre introduit en résumé la méthode d'optimisation qui est utilisée afin de résoudre le problème inverse de conduction de chaleur. L'application de la technique d'optimisation nous donne une possibilité de résoudre facilement un tel problème. La méthode d'optimisation par gradient conjugué nous apporte un algorithme de solution pour le problème présenté. En introduisant la dérivation du problème de sensibilité et du problème adjoint, ce chapitre présente aussi une analyse de sensibilité et d'autres aspects de cette solution.

Le troisième chapitre présente l'implémentation numérique de cet algorithme de solution.

Le quatrième chapitre présente, à partir de cas différents, les résultats obtenus et les discussions relatives au problème direct ainsi qu'inverse de conduction de chaleur. Des résultats raisonnables pour le problème inverse de conduction de chaleur peuvent être obtenus en utilisant la méthode introduite, et en déplaçant la frontière avec une vitesse imposée indépendamment de la température ou déterminée comme une partie de la

solution du problème inverse. Les valeurs de la solution inverse sont proches des valeurs réelles. En considérant des données comportant du bruit aléatoire, l'écart entre les valeurs réelles et celles provenant de la solution inverse est devenu un peu plus grand. Dans certains cas, De meilleurs résultats peuvent être obtenus par l'augmentation du nombre d'itérations.

La conclusion et les recommandations pour les travaux de recherche à venir sont présentés dans la conclusion.

Nous avons constaté que l'approche de résolution de ce problème inverse de conduction de chaleur est généralisable aux autres domaines d'ingénierie.

ABSTRACT

This thesis introduces the method for solving an inverse heat conduction problem with a moving boundary, by conjugate gradient method, with adjoint equation. This approach requires the derivation of three sets of coupled equations, namely, direct equation, sensitivity equation and adjoint equation.

The derivations of governing equations in dimensionless form are given in Chapter I. The direct problem solution is the foundation of the inverse problem. The description for the direct heat conduction problem is given in this chapter, as well as the inverse heat conduction problem.

Chapter II concisely introduces the optimization method which are used in solving the inverse heat conduction problem. The application of optimization techniques makes it possible to solve the inverse problem easily. The technique of optimization by the conjugate gradient method leads to a solution algorithm for the inverse problem of heat conduction.

The sensitivity problem and adjoint problem are described respectively in this chapter. The derivation of the sensitivity equation and adjoint equation are also provided.

Chapter III describes the numerical implementation of the algorithm of solution.

Chapter IV provides the results and discussions for the direct heat conduction and the inverse heat conduction problem (IHCP) in different cases. The reasonable results of inverse conduction problem can be obtained with the introduced method when the boundary is moving with a velocity imposed independently from the temperature field or determined as part of the solution of the inverse problem. The inverse solution value is close to actual value. But when noisy data is considered, the discrepancy between the

actual and inverse values become bigger. For some cases, better results can be obtained by increasing the number of iterations.

The brief conclusion of research and recommendation for future work are given in the conclusion.

It is found that the ideas for solving the inverse heat conduction may be extended to much wider fields in practical engineering.

CONDENSÉ EN FRANÇAIS

L'analyse générale d'un problème de conduction procède à partir de conditions limites données à la cherche d'une solution pour une série d'équations décrivant la physique réelle du transfert de chaleur. Elle requiert aussi une condition initiale si le problème est transitoire. Elle est connue comme le problème standard et direct de transfert de chaleur. Dans la plupart des situations pratiques, les conditions de frontière restent souvent inconnues en majorité, tandis que la valeur de la température interne est plus pratique à mesurer, ou soit décrit optimalement dans le design. Dans ce cas, il est nécessaire d'avoir recours au concept du problème inverse [1]. Le problème inverse de conduction de chaleur est défini comme la recherche de l'évolution du flux de chaleur à la surface, en se basant sur l'évolution de températures mesurées à l'intérieur du corps conducteur de chaleur.

L'approche inverse, au contraire de celle en direct, essaie de prévoir les conditions thermiques de la frontière à partir des données expérimentales, surtout celles mesurées ou obtenues dans le champ de température.

Le problème de transfert inverse de chaleur devient de plus en plus important dans la société industrielle moderne. Présentement, beaucoup de domaines en haute technologie rencontrent des problèmes de transfert inverse de chaleur tel que la procédure de design pour le chauffage, la congélation, le moulage et la fonte, la détermination des coefficients de transfert de chaleur, le domaine aérospatial, etc. À la suite du développement de la méthode mathématique et de la technologie informatique, ce type de problème a retenu l'attention, et il nous est maintenant possible, plus que jamais, de résoudre les problèmes de transfert inverse de chaleur.

L'histoire du problème inverse de conduction de chaleur n'est pas aussi longue que celle des autres problèmes de conduction de chaleur. Ce n'est seulement depuis le dix-

neuvième siècle, que le problème inverse de conduction de chaleur a suscité intérêt croissant tant en théorie qu'en pratique sur la procédure de transfert de chaleur. Par exemple, l'étude de transfert transitoire de chaleur sur des phénomènes associés avec la navette spatiale dans le domaine aéronautique, la recherche de propriétés des matériaux, le contrôle d'une procédure de solidification, etc.

Il existe certains facteurs qui excitent l'intérêt des scientifiques et des ingénieurs pour résoudre ce type de problème. Ces facteurs peuvent se résumer comme suit :

1. À la suite du développement de la science et de la technologie, beaucoup de problèmes inverses de conduction de chaleur ont été rencontrés. L'un des joyaux de haute technologie, la navette spatiale et la fusée sont lancées pour des buts différents. Afin d'augmenter la fiabilité de la navette et de la fusée, le champ de température à la surface extérieure doit être obtenu. Nous ne pouvons pas, malheureusement, mesurer la température à surface extérieure du véhicule. Seule la température à l'intérieur du véhicule peut être mesurée. C'est là un problème inverse de conduction de chaleur. Nous rencontrons aussi des problèmes inverses de conduction de chaleur durant le diagnostic, le design, le contrôle dans les différents systèmes d'ingénierie.

2. Les méthodes mathématiques nécessaires ont été rendues disponibles. La technique d'optimisation, par exemple, a été développée au siècle dernier. Ces avancements dans le domaine mathématique nous fournissent des idées afin de résoudre ce type de problème et d'avoir une solution raisonnable.

3. La révolution du calcul numérique au milieu du siècle dernier, suite à l'avènement d'ordinateurs modernes. Il est possible maintenant de résoudre le problème inverse de conduction de chaleur.

En conclusion, à la suite du développement de la technologie, beaucoup de problèmes inverses sont apparus de plus en plus souvent dans le domaine d'ingénierie thermique. Et il nous est impossible de les éviter. Nous devons déterminer les états du système et les causes qui génèrent ces états telles que les propriétés thermophysiques, etc. Le développement de méthodes mathématiques et informatiques nous donnent la possibilité d'avoir une solution remarquable pour les problèmes inverses de conduction de chaleur.

Dans ce mémoire, incluant l'étude d'une frontière en mouvement, le problème inverse de conduction de chaleur à une dimension a été discuté en détails, à partir de la mesure de température au milieu du domaine. Pour ce problème, quand les valeurs discrètes de la courbe de flux q sont considérées, l'optimisation des résultats requiert des étapes temporelles plus petites. Tandis qu'une étape temporelle petite cause souvent l'instabilité de la solution de ce problème à l'exception du cas de l'emploi de restrictions. Alors, un problème inverse de conduction de chaleur est plus difficile à résoudre numériquement qu'un problème direct. Dans ce mémoire, il est présumé que l'information a priori concernant la forme de surface sera disponible. La vitesse doit être prédécrite ou déterminée par le gradient de température local. Un algorithme, qui contient tant les équations de sensibilité que les équations adjointes, a été présenté. Toutes les équations sont transformées dans un système de coordonnées sans dimension. La procédure de discrétisation pour le contrôle implicite de volume, basée sur le schéma power-law de Patankar [48], est exposée en détails.

La technique d'optimisation de la méthode du gradient conjugué est appliquée à résoudre ce problème inverse. Elle comporte trois équations, c'est-à-dire l'équation directe, l'équation de sensibilité, l'équation adjointe.

L'introduction expose un résumé sur le problème inverse de conduction de chaleur et les développements les plus récents de ce problème.

Le premier chapitre présente les équations gouvernantes.

Le deuxième chapitre présente la méthode d'optimisation, qui est utilisé dans les travaux de ce mémoire dans le but de résoudre le problème inverse de conduction de chaleur.

Le troisième chapitre décrit l'implémentation numérique et présente l'algorithme de solution.

Le quatrième chapitre présente les solutions selon des conditions différentes à la frontière, et aussi les résultats obtenus et les discussions pertinentes.

La conclusion et les recommandations pour les travaux de recherche à venir sont présentés dans la conclusion.

TABLE OF CONTENTS

DEDICACE.....iv

ACKNOWLEDGEMENT.....v

RÉSUMÉ.....vi

ABSTRACT.....viii

CONDENSÉ EN FRANÇAIS..... x

TABLE OF CONTENTS.....xiv

LIST OF FIGURES.....xvi

LIST OF SYMBOLS.....xxii

INTRODUCTION.....1

0.1 Literature review.....3

0.2 Outline of thesis.....5

CHAPTER I MATHEMATICAL FORMULATION.....7

1.1 Governing equations and dimensionless variables.....7

1.2 Direct problem and inverse problem.....9

1.2.1 Direct problem.....9

1.2.2 Inverse problem.....10

CHAPTER II OPTIMIZATION METHOD.....13

2.1 Optimization approach.....13

2.2 Application of optimization method.....14

2.3 Equation of sensitivity.....17

2.4 Adjoint equation.....18

2.5 Minimization algorithm.....23

CHAPTER III NUMERICAL IMPLEMENTATION.....26

3.1 Discretization of the equations 26

3.2 Algorithm of solution 31

CHAPTER IV RESULTS AND DISCUSSIONS.....33

4.1 Direct heat conduction problem 33

4.2 Inverse heat conduction problem.....42

CONCLUSION.....68

REFERENCES.....71

LIST OF FIGURES

Figure 1.1 Geometry and boundary conditions.....7

Figure 3.1 Grid System of the Problem.....27

Figure 3.2 Control volume for internal node.....29

Figure 4.1 Direct Solution for Case 1 q =-1, V= 1.....34

Figure 4.2 Direct Solution for Case 2 q =-t, V= 1.....34

Figure 4.3a Direct Solution for Case 3-1 q =-sin (ωt), V= 1, ω =1.....35

Figure 4.3b Direct Solution for Case 3-2 q =-sin (ωt), V= 1, ω =10.....35

Figure 4.4 Direct Solution for Case 4 q =-1, V= -dT/dxlx=L.....35

Figure 4.5 Direct Solution for Case 5 q =-t, V= -dT/dxlx=L.....36

Figure 4.6a Direct Solution for Case 6-1 q =-sin (ωt), V= -dT/dxlx=L, ω =1.....36

Figure 4.6b Direct Solution for Case 6-2 q =-sin (ωt), V= -dT/dxlx=L, ω =10.....36

Figure 4.7 Direct Solution for Case 7 q =-1, V= sin (ωt), ω = 1.....37

Figure 4.8 Direct Solution for Case 8 q =-t, V= sin (ωt), ω = 1.....37

Figure 4.9a Direct Solution for Case 9-1 q =-sin (ωt), V= sin (ωt), ω = 1.....37

Figure 4.9b Direct Solution for Case 9-2 q =-sin (ω1*t) V= sin (ω2*t) ω1 = 10, ω2 =1.....38

Figure 4.10 Isotherm Case 3-1 At tf for q =-sin (ωt), V= 1, ω = 1.....38

Figure 4.11 Direct Solution Case 3-1 q =-sin (ωt), V= 1, ω =1.....38

Figure 4.12 Isotherm for Case 3-2 At tf for q =-sin (ωt), V= 1, ω = 10.....39

Figure 4.13 3-D Temperature Field for Case 3-2 q =-sin (ωt), V= 1, ω = 10.....39

Figure 4.14 Isotherm for Case 9-1 At tf q =-sin (ω1*t), V= sin (ω2*t), ω1 = 1, ω2 = 1.....39

Figure 4.15 Direct Solution for Case 9-1 q =-sin (ω1*t), V= sin (ω2*t) ω1 = 1, ω2 = 1.....39

Figure 4.16: Isotherm Case 9-2 At tf q =-sin (ω1*t), V=sin (ω2*t) ω1 = 10,ω2=1....40

Figure 4.17: 3-D Temperature Field for Case 9-2 q =-sin (ω1*t), V= sin (ω2*t)
ω1 = 10, ω2 = 1 40
Figure 4.18: Heat Flux Vs Time for Case 1 q =-1, V= 1 42
Figure 4.19: Inverse Solution of Heat Flux for Case 1 q =-1, V= 1 and Sigma=0.001...42
Figure 4.20: Inverse Solution of Heat Flux for Case 1 q =-1, V= 1 and Sigma=0.04....42
Figure 4.21: Interface Position Vs Time for Case 1 q =-1, V= 1 43
Figure 4.22: Contrast Between Direct Solution and Inverse Solution of Temperature
for Case 1 q =-1, V= 1 43
Figure 4.23: 3-D Inverse Solution Case 1 q =-1, V= 1 43
Figure 4.24: Error Evolution for Case 1 q =-1, V= 1 43
Figure 4.25: Heat Flux Vs Time for Case 2 q =-t, V= 1 44
Figure 4.26: Inverse Solution of Heat Flux for Case 2 q =-t, V= 1 and Sigma=0.001...45
Figure 4.27: Inverse Solution of Heat Flux for Case 2 q =-t, V= 1 and Sigma=0.04.....45
Figure 4.28: Interface Position Vs Time for Case 2 q =-t, V= 1 45
Figure 4.29: Contrast Between Direct Solution and Inverse Solution of Temperature
for Case 2 q =-t, V= 1at t=tf 45
Figure 4.30: 3-D Inverse Solution for Case 2 q =-t, V= 1 46
Figure 4.31: Error Evolution for Case 2 q =-t, V= 1 46
Figure 4.32: Heat Flux Vs Time for Case 3-1 q =-sin (ω*PI*t), V= 1, ω = 1 46
Figure 4.33: Inverse Solution of Heat Flux for Case 3-1 q =-sin (ω*PI*t), V= 1, ω = 1,
Sigma=0.001 47
Figure 4.34: Inverse Solution of Heat Flux for Case 3-1 q =-sin (ω*PI*t), V= 1, ω = 1,
Sigma=0.04 47
Figure 4.35: Interface Position Vs Time for Case 3-1 q =-sin (ω*PI*t), V= 1, ω = 1....47
Figure 4.36: Contrast Between Direct Solution and Inverse Solution of Temperature
for Case 3-1 q =-sin (ω*PI*t), V= 1, ω = 1 47
Figure 4.37: 3-D Inverse Solution for Case 3-1 q =-sin (ω*PI*t), V= 1, ω = 1 48
Figure 4.38: Error Evolution for Case 3-1 q =-sin (ω*PI*t), V= 1, ω = 1 48

Figure 4.39: Heat Flux Vs Time for Case 3-2 q =-sin (ω*PI*t), V= 1, ω = 10, Iteration=19.....49
Figure 4.40: Heat Flux Vs Time for Case 3-2 q =-sin (ω*PI*t), V= 1, ω = 10, Iteration=40.....49
Figure 4.41: Heat Flux Vs Time for Case 3-2 q =-sin (ω*PI*t), V= 1, ω = 10, Iteration=100.....49
Figure 4.42: Interface Position Vs Time for Case 3-2 q =-sin (ω*PI*t), V= 1, ω = 10...50
Figure 4.43: Contrast Between Direct Solution and Inverse Solution of Temperature for Case 3-2 q =-sin (ω*PI*t), V= 1, ω = 10.....50
Figure 4.44: 3-D Inverse Solution for Case 3-2 q =-sin (ω*PI*t), V= 1, ω = 10.....50
Figure 4.45: Error Evolution for Case 3-2 q =-sin (ω*PI*t), V= 1, ω = 10.....50
Figure 4.46: Heat Flux Vs Time for Case 4 q =-1, V= -dT/dxlx=L.....51
Figure 4.47: Inverse Solution of Heat Flux for Case 4 q =-1, V= -dT/dxlx=L, Sigma=0.001.....52
Figure 4.48: Inverse Solution of Heat Flux for Case 4 q =-1, V= -dT/dxlx=L, Sigma=0.04.....52
Figure 4.49: Interface Position Vs Time for Case 4 q =-1, V=- dT/dxlx=L.....52
Figure 4.50: Contrast Between Direct Solution and Inverse Solution of Temperature for Case 4 q =-1, V= -dT/dxlx=L.....52
Figure 4.51: 3-D Inverse Solution for Case 4 q =-1, V= -dT/dxlx=L.....53
Figure 4.52: Error Evolution for Case 4 q =-1, V= -dT/dxlx=L.....53
Figure 4.53: Heat Flux Vs Time for Case 5 q =-t, V= -dT/dxlx=L.....53
Figure 4.54: Inverse Solution of Heat Flux for Case 5 q =-t, V=- dT/dxlx=L, Sigma=0.001.....54
Figure 4.55: Inverse Solution of Heat Flux for Case 5 q =-t, V=- dT/dxlx=L, Sigma=0.04.....54
Figure 4.56: Interface Position Vs Time for Case 5 q =-t, V= -dT/dxlx=L.....54
Figure 4.57: Contrast Between Direct Solution and Inverse Solution of Temperature for Case 5 q =-t, V= -dT/dxlx=L.....54

Figure 4.58: 3-D Inverse Solution for Case 5 q =-t, V=- dT/dxlx=L.....55
Figure 4.59: Error Evolution for Case 5 q =-t, V= -dT/dxlx=L.....55
Figure 4.60 Heat Flux Vs Time for Case 6-1 q =-sin (ω*PI*t),
V=- dT/dxlx=L ω = 1.....55
Figure 4.61: Inverse Solution of Heat Flux for Case 6-1 q =-sin (ω*PI*t),
V= -dT/dxlx=L, ω = 1, Sigma=0.001.....56
Figure 4.62: Inverse Solution of Heat Flux for Case 6-1 q =-sin (ω*PI*t),
V= -dT/dxlx=L, ω = 1, Sigma=0.04.....56
Figure 4.63: Interface Position Vs Time for Case 6-1 q =-sin (ω*PI*t),
V= -dT/dxlx=L, ω = 1.....56
Figure 4.64: Contrast Between Direct Solution and Inverse Solution of Temperature
for Case 6-1 q =-sin (ω*PI*t), V= -dT/dxlx=L, ω = 1.....56
Figure 4.65: 3-D Inverse Solution for Case 6-1 q =-sin (ω*PI*t), V= -dT/dxlx=L,
ω = 1.....57
Figure 4.66: Error Evolution for Case 6-1 q =-sin (ω*PI*t), V=- dT/dxlx=L, ω = 1....57

Figure 4.67: Heat Flux Vs Time for Case 6-2 q =-sin (ω*PI*t), V= -dT/dxlx=L,
ω = 10.....57
Figure 4.68: Interface Position Vs Time for Case 6-2 q =-sin (ω*PI*t),
V= -dT/dxlx=L, ω = 10.....58
Figure 4.69: Contrast Between Direct Solution and Inverse Solution of Temperature
for Case 6-2 q =-sin (ω*PI*t), V= -dT/dxlx=L, ω = 10.....58
Figure 4.70: 3-D Inverse Solution for Case 6-2 q =-sin (ω*PI*t), V= -dT/dxlx=L,
ω = 10.....58
Figure 4.71: Error Evolution for Case 6-2 q =-sin (ω*PI*t), V= -dT/dxlx=L,
ω = 10.....58
Figure 4.72: Heat Flux Vs Time for Case 7 q =-1, V= sin (ωt), ω = 1.....59
Figure 4.73: Inverse Solution of Heat Flux for Case 7 q =-1, V= sin (ωt), ω = 1,

Sigma=0.001.....59
Figure 4.74: Inverse Solution of Heat Flux for Case 7 q =-1, V= sin (ωt), ω = 1, Sigma=0.04.....59
Figure 4.75: Interface Position Vs Time for Case 7 q =-1, V= sin (ωt), ω = 1.....60
Figure 4.76: Contrast Between Direct Solution and Inverse Solution of Temperature for Case 7 q =-1, V= sin (ωt), ω = 1.....60
Figure 4.77: 3-D Inverse Solution for Case 7 q =-1, V= sin (ωt), ω = 1.....60
Figure 4.78: Error Evolution for Case 7 q =-1, V= sin (ωt), ω = 1.....60
Figure 4.79: Heat Flux Vs Time for Case 8 q =-t, V= sin (ωt), ω = 1.....61
Figure 4.80: Inverse Solution of Heat Flux for Case 8 q =-t, V= sin (ωt), ω = 1, Sigma=0.001.....61
Figure 4.81: Inverse Solution of Heat Flux for Case 8 q =-t, V= sin (ωt), ω = 1, Sigma=0.04.....61
Figure 4.82: Interface Position Vs Time for Case 8 q =-t, V= sin (ωt), ω = 1.....62
Figure 4.83: Contrast Between Direct Solution and Inverse Solution of Temperature for Case 8 q =-t, V= sin (ωt), ω = 1.....62
Figure 4.84: 3-D Inverse Solution for Case 8 q =-t, V= sin (ωt), ω = 1.....62
Figure 4.85: Error Evolution for Case 8 q =-t, V= sin (ωt), ω = 1.....62
Figure 4.86: Heat Flux Vs Time for Case 9-1 q =-sin (ω*PI*t), V= sin (ωt), ω = 1.....63
Figure 4.87: Inverse Solution of Heat Flux for Case 9-1 q =-sin (ω*PI*t), V= sin (ωt), ω = 1, Sigma=0.001.....63
Figure 4.88: Inverse Solution of Heat Flux for Case 9-1 q =-sin (ω*PI*t), V= sin (ωt), ω = 1, Sigma=0.04.....63
Figure 4.89: Interface Position Vs Time for Case 9-1 q =-sin (ω*PI*t), V= sin (ωt), ω = 1.....64
Figure 4.90: Contrast Between Direct Solution and Inverse Solution of Temperature for Case 9-1 q =-sin (ω*PI*t), V= sin (ωt), ω = 1.....64
Figure 4.91: 3-D Inverse Solution for Case 9-1 q =-sin (ω*PI*t), V= sin (ωt),

ω = 1.....64
Figure 4.92: Error Evolution for Case 9-1 q =-sin (ω*PI*t), V= sin (ωt), ω = 1.....64
Figure 4.93: Heat Flux Vs Time for Case 9-2 q =-sin (ω1*PI*t),
V= sin (ω2*t) ω1 = 10, ω2 = 1, iteration=19.....65
Figure 4.94: Inverse Solution of Heat Flux for Case 9-2 q =-sin (ω1*PI*t),
V= sin (ω2*t), ω1 = 10, ω2 =1,iteration=40.....65
Figure 4.95: Inverse Solution of Heat Flux for Case 9-2 q =-sin (ω1*PI*t),
V= sin (ω2*t), ω1 = 10, ω2 = 1, iteration=100.....65
Figure 4.96: Interface Position Vs Time for Case 9-2 q =-sin (ω1*PI*t), V= sin (ω2*t)
ω1 = 10, ω2 = 1.....66
Figure 4.97: Contrast Between Direct Solution and Inverse Solution of Temperature
for Case 9-2 q =-sin (ω1*PI*t), V= sin (ω2*t) ω1 = 10, ω2 = 1.....66
Figure 4.98: 3-D Inverse Solution for Case 9-2 q =-sin (ω1*PI*t), V= sin (ω2*t)
ω1 = 10, ω2 = 1.....66
Figure 4.99: Error Evolution for Case 9-2 q =-sin (ω1*PI*t), V= sin (ω2*t)
ω1 = 10, ω2 = 1.....66

LIST OF SYMBOLS

b	source term
D	considered domain
E	object functional of optimization
H	width of the region studied
I	node position along x coordinate
J	node position along y coordinate
J_x, J_y	intermediate variable
k	thermal conductivity, $W/(m \cdot K)$
L_0	length of studied region, m
L	dimensionless length of studied region
n	normal direction
p	optimization direction
q	heat flux
Q_{ref}	reference flux value
$\vec{r}$	position vector, m
S	surface
t	time, s
T	temperature, K
T_m	measured temperature
ΔT	temperature scale
x, y	coordinates
Δx	mesh size along x
Δy	mesh size along y

Greek symbols

α	thermal diffusivity or optimal step size of conjugate gradient
β	thermal dilatational coefficient
Δ	increment
ρ	mass density
ϕ	arbitrary function
∇	gradient operator
$\nabla\cdot$	divergence operator
∇^2	Laplacian operator

Superscripts

$\bar{}$	adjoint variables
$\sim$	sensitivity variables
k	iteration step

Subscripts

i	node series number in x coordinate
j	node series number in y coordinate
m	measured value or boundary
max	maximum value

INTRODUCTION

The usual analysis of a conduction problem proceeds from the given boundary conditions to seek a solution to the set of governing equations describing the actual physics of heat transfer. It also requires an initial condition, if the process is transient. This is known as a standard, direct heat transfer problem. In many practical situations, boundary conditions are often the major unknowns, while internal temperature values are either more conveniently measured, or are optimally prescribed by design. In such cases, it is necessary to rely on the inverse problem concept[1]. The inverse heat conduction problem is defined as follows: The IHCP is the estimation of the surface heat flux history given one or more measured temperature histories inside a heat-conducting body.

The inverse approach, in contrast with the direct one, seeks to predict the thermal boundary conditions from the experimental data, namely measured temperatures obtained within the temperature field.

The inverse heat transfer problem has become more and more important in the modern Industry society. Now lots of fields in high technology encounter inverse heat transfer problems, such as heating and cooling, casting and melting process design, determination of convective heat transfer coefficients, the field of aerospace and so on. With the development of mathematical methods and the computer technology, this kind of problems has been paid attention to, and it is now possible for us to solve inverse heat transfer problems.

The history of the inverse heat transfer problem is not as long as that of other heat transfer problems. Only since the nineteenth century, has the inverse heat transfer problem received an increasing interest in the theory and applications of heat transfer processes. For example, the study of transient heat transfer phenomena associated with

re-entry aircraft in aerospace field[2,3,4], the research of the properties of materials in material field [5,6,7], the control of solidification processes [8,9,10,11,12,13,14] and so on.

There are several kinds of facts [15] which have led scientists and engineers to give much more effort to solve this kind of problems. The facts are as follows below:

1. With the development of science and technology, lots of inverse heat transfer problem are encountered. One of the milestones of high technology, the shuttle and rocket are launched for different purposes. In order to improve the reliability of shuttle and rocket, the temperature field of outer surface of vehicle must be obtained. We can not, however, measure the temperature of the outer surface of the vehicle. Only the temperature in the vehicle can be measured. This is an inverse heat transfer problem. We also encounter inverse problem in diagnostic, design and control in the various system in practical engineering.

2. The necessary mathematical methods were available. The optimization method, for instance, has been developed in last century. These achievements in mathematical methods provide the ideas for solving this kind of problem and make the solution of ill-posed problems reasonable.

3. The revolution of calculation in the middle of the last century, provided the invention of the computer as a powerful calculation tool. This great invention makes it possible to solve the inverse heat transfer problem. This is because the process of solving inverse heat transfer problem requires complicated analysis and tremendous calculations.

In conclusion, with the development of technology, so many inverse problems are arising in practical thermal engineering, that it is simply impossible to avoid them. We

have to determine the state of systems, the causes leading to these states, such as thermophysical properties and so on. But the development of mathematical methods and computational tools make it possible to obtain meaningful solutions to the inverse heat transfer problems.

0.1 Literature review

The first attempt to solve an inverse heat transfer problem was related to the determination of historical climate and thermal conductivity of earth's ground layer. Stefan obtained an infinite series solution to inverse heat conduction in 1890[1]. This result is the first exact solution of a one-dimensional inverse heat transfer problem. One of the earliest papers on the inverse heat conduction problem (IHCP) was published by Stolz[16] in 1960. It addressed calculation of heat transfer rates during quenching of bodies of simple finite shapes. Stolz claimed use of his method as early as June 1957. For semi-infinite geometries Mirsepassi[17] maintained that he had used the same technique both numerically and graphically[18] for several years prior to 1960. A Russian paper by Shumakov[19] on the IHCP was translated in 1957. The space program, starting about 1956, gave considerable impetus to the study of the inverse heat conduction problem. The applications therein were related to nose cones of missiles and probes, to rocket nozzles, and other devices. Beck also initiated his work on the IHCP about that time and developed the basic concepts [20,21,22,23,24,25,26] that permitted much smaller time steps than the Stolz method. Others whose work had application to the space program included Blackwell [27,28], Mulholland[29,30,31,32], and Williams and Curry[33]. Another research area that extensively required solutions of the IHCP was the testing of nuclear reactor components. Many of the computer programs in current use in the United States appear to be based on the method described in a 1970 paper [24]. Other applications reported for the IHCP included:

1) Periodic heating in combustion chambers of internal combustion engines

2) Solidification of glass

3) Indirect calorimetry for laboratory use

4) Transient boiling curve studies

There have been extremely varied approaches to the inverse heat conduction problem. These have included the use of Duhamel's theorem (or convolution integral) which is restricted to linear problems. Numerical procedures such as finite differences and finite elements have also been employed due to their inherent ability to treat nonlinear problems. Exact solution techniques were proposed by Burggraf[34] and Khan[35], Langford[36], and others; such techniques have limited use for realistic problems, but they can give considerable insight into the IHCP. Some techniques used Laplace transforms and were also limited to linear cases.

The IHCP is one of many mathematically "ill-posed" problems. This means that the inherent errors, however small, of internal measured data may result in an unrealistic and unstable prediction of boundary condition, making the solution extremely sensitive to measurement errors. Such problems are typical of inverse solutions. There are a number of procedures that have been advanced for the solution of ill-posed problems in general. One of these was developed by Tikhonov and Arsenin in 1963[37]. Tikhonov introduced what he called the regularization method to reduce the sensitivity of ill-posed problems to measurement errors. A modification of this method is presented herein for more efficient solution of the IHCP. Numerous other general procedures for ill-posed problems have been proposed including a technique, well known to geophysicists, called the Backus-Gilbert technique [38,39,40]. The mathematical techniques for solving sets of ill-conditioned algebraic equations called single-value decomposition techniques can also be used for the IHCP.

For the one-dimensional IHCP when discrete values of the q curve are estimated, maximizing the amount of information implies small time steps. But the small time

steps frequently cause instabilities in the solution of IHCP unless restrictions are employed. Hence, the inverse heat transfer problem is much harder to solve analytically than the direct problem.

In this project, a one-dimensional IHCP with moving-boundary is discussed in detail, as might be found, from temperature measurements in the middle of media. In this project, it is assumed that a priori information about the form of the interface is available. The velocity might be prescribed or determined from the local temperature gradient. A solution algorithm is presented, which involves both a sensitivity equation and an adjoint equation. All the equations are transformed in dimensionless coordinate. The implicit control volume discretization procedure, based on power-law scheme of Patankar[48], is exposed in details.

The optimization technique of the conjugate gradient method, is applied to solve this inverse problem, which consists of a set of three equations, i.e. direct equation, sensitivity equation and adjoint equation.

0.2 Outline of thesis

This thesis is devoted to the Simulation of Inverse Conduction with a Moving Boundary.

One of the main motivations for this research lies in the belief that inverse heat transfer problem are of prime importance in a wide range of applications. For example, advanced technologies in medicine, aeronautics and microelectronics.

In order to facilitate the reading of the rest of this thesis, we present here a brief description of contents of the following chapters.

In Chapter I, the governing equations are presented.

The optimization method used in this thesis to solve the inverse heat transfer problem is introduced in detail in Chapter II.

The sensitivity equation and adjoint equation are also introduced and derived in this chapter

Chapter III describes numerical implementation and gives the algorithm of solution.

The chapter IV provides the solutions for different boundary conditions .The results and discussions are given in this chapter.

The brief conclusion and recommendation for the future research are given in the conclusion.

CHAPTER I

MATHEMATICAL FORMULATION

1.1 Governing equation and dimensionless variables

For solving the inverse problem, the thermal behavior of the real system (physical model) should be described by a mathematical model. The mathematical model may be described either by partial differential equations or ordinary differential equations. For the solution of the mathematical model, two kinds of approximation are implied. One is the simplification in the physical model of the real system. The other one is the approximation which is related to the method of solution.

In this thesis, the accuracy and stability of the solution obtained by the conjugate gradient are discussed in detail.

Let us consider the inverse heat conduction problem sketched in Fig.1.1

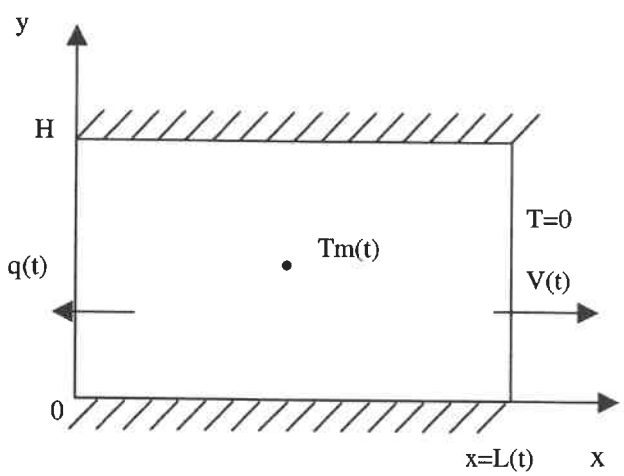

Figure 1.1 Geometry and boundary conditions

In the definition of the problem, the domain is a rectangular cavity with top and bottom faces insulated. The problem is one-dimensional without any y-dependency. Therefore

the flux imposed on the boundary at $x = 0$ or $x = L$ is of the form $q(t)$ and the temperature field can only be $T(x,t)$.

The main purpose in this thesis is to determine the unsteady flux $q(t)$ at $x = 0$ over the time interval $0 \le t \le t_f$, from temperature measurements Tm, taken at the sensor position, which is at the middle point of the domain.

In order to simplify equations and gain more universality, the IHCP may be expressed in a convenient non-dimensional form by introducing the definitions:

$$
\begin{aligned}
T^* &= \frac{T - T_0}{\Delta T} \\
\Delta T &= \frac{Q_{ref} * L}{k} \\
x^* &= \frac{x}{L} \\
t^* &= \frac{\alpha t}{L^2}
\end{aligned}
\tag{1.1}
$$

where T ~ temperature

Q_{ref} ~ reference flux value

L ~length

α ~ thermal diffusivity

k ~ conductivity

All properties are evaluated at T_0 . Omitting superscripts from now on, the temperature field within the cavity satisfies the unsteady dimensionless heat equation:

$$\frac{\partial T}{\partial t} = \nabla^2 T \tag{1.2}$$

This is the dimensionless governing equation of the direct problem.

1.2 Direct problem and inverse problem

1.2.1 Direct problem

The direct techniques are the first stage of solution procedures for the inverse heat problem. We have had many mature methods to solve direct problems. Partial differential equations describing the physical phenomena of heat conduction can be solved using a variety of methods, including exact and numerical procedures. The exact methods include the classical methods of separation of variables and Laplace transforms. One is based on an integral formulation of the mathematical model and the other on a differential form of the model. In general, the equations describing heat conduction are nonlinear. The solution of a nonlinear heat conduction problem requires an approach that discretizes the partial differential equations. Two methods for solving the nonlinear heat conduction equation are the finite difference and finite element (FE) methods. In this thesis, the finite difference method is used in which conservation of energy is applied directly to finite control volumes; it is called the finite control volume procedure.

If the boundary conditions are completely given, we are dealing with a direct problem.

For the situation discussed here, we have the following boundary conditions.

$$T(L,t) = 0 \qquad \text{at} \quad x = L \tag{1.3}$$

$$k\frac{\partial T(0,t)}{\partial x} = q(t) \qquad \text{at} \quad x = 0 \tag{1.4}$$

$$V(t) = \begin{cases} b(t) \\ -\dfrac{\partial T}{\partial x} \end{cases} \qquad \text{at} \quad x = L \tag{1.5}$$

where, $b(t)$ is known if velocity is given.

For the initial condition, a constant temperature is assumed, namely

$$T = 0 \qquad \text{at} \quad t = 0 \tag{1.6}$$

According to these conditions, the solution of the governing equation ,i.e ,the temperature distribution $T(x,t)$ in the domain $0 \le x \le L$ during the interval $0 \le t \le t_{\max}$ can be determined.

1.2.2 Inverse Problem

During the past two decades, the special case of estimating a surface condition from interior measurements has come to be known as the inverse heat conduction problem. There are numerous other inverse problems in transient conduction and diffusion [1]. Although the formulation and solution of this problem were presented over a century ago, its development has rapidly grown only during the last twenty years, due to a combination of the advent of high technologies, new mathematical achievements and modern computational facilities.

The inverse heat conduction problem is much more difficult to solve analytically than the direct problem. But in the direct problem many experimental impediments may arise

in measuring or producing given boundary conditions. The physical situation at the surface may be unsuitable for attaching a sensor, or the accuracy measurement may be seriously impaired by the presence of the sensor. Although it is often difficult to measure the temperature history of the heated surface of a solid, it is easier to measure accurately the temperature history at an interior location or at an insulated surface of the body. Thus, there is a choice between relatively inaccurate measurements or a difficult analytical problem. An accurate and tractable inverse problem solution would thus minimize both disadvantages at once [1].

Most research until now was, however, devoted to the basic one-dimensional inverse heat conduction problem, to understand the ill-posed nature of the problem, and to devise solution methods that would ensure stability, even at the expense of a slight loss of accuracy.

An overall and systematical review of the IHCP is provided in the book of Beck et al.[1] and Alifanov, which present the solution techniques falling into two main categories, namely, the sequential function specification method, pioneered by Beck, and the function estimation method, developed by Alifanov, Tikhonov, and other reseachers in Russia. The former method relies on the concept of future times to achieve stability. The latter is based on error optimization over the whole time domain, by a descent method of some sort, conjugate gradient or otherwise.

Suppose from now on that a temperature sensor is located in the middle of the field. The measurements at the sensor are available, and there is no information about temperature and flux at the fixed boundary($x = 0$ over $0 \le t \le t_{\max}$).

Our purpose is to recover $q(t)$ at $x = 0$ from the temperature measurements to satisfy equation (1.2) and the boundary equations during the period $0 \le t \le t_{\max}$.

This is a 1-D inverse heat conduction problem. Normally, there are two methods for solving this kind of inverse problem. One is space marching method and the other one is conjugate gradient method. In fact, when used in conjunction with an appropriate mollification technique, the space marching technique is very fast to provide a regularized albeit distored solution, while the iterative conjugate gradient technique proves to be slow, but robust and more available. Here, we will focus the conjugate gradient method.

CHAPTER II

OPTIMIZATION METHOD

2.1 Optimization approach

In order to solve the inverse problem of heat transfer, various techniques have been proposed, e.g., the space marching, the perfect matching, the digital filtering, the future time stepping, etc. A review of these techniques was given in the book of Beck, Blackwell and St. Clair Jr. These different techniques may be broadly classified into two categories, namely, the sequential method and the whole time domain method. While the first method was proposed by Beck in the U.S., the second one was actively promoted by Tikhonov in the U.R.S.S. A recent comparative study of these two methods by Beck indicated that while the former is fast, the latter is robust, and a hybird method might be a success.

In the following paragraphs, we will give the steps of a method of solution to the inverse conduction problem for the case where no a priori information is available of the unknown boundary heat flux.

The proposed method treats the inverse problem from an optimization point of view[42]. To solve the inverse conduction problem, let us consider conjugate gradient methods(CGM).

A very desirable feature of conjugate direction methods is that only function and gradient values of the objective function are required for their implementation. Consequently conjugate direction methods may be used to estimate a minimizer X^* of a non-quadratic as well as a quadratic objective function f without having to compute the second partial derivatives of f. Convergence will not in general be obtained in a

finite number of iterations if f is not quadratic, and the number of iterations required to attain a given accuracy depends upon the initial estimate X^0 of X^* [43].

Because the conjugate gradient method has been used extensively to solve many kinds of inverse problems [44,45,46,47], including IHCP, as well as problems of parameters determination and shape identification, it is very meaningful to discuss how a solution is constructed via this algorithm.

The conjugate gradient method will be used exclusively in solving one dimensional IHCP in this thesis. The results will demonstrate the sequential recovery of unknown heat flux with different frequency components. The lower frequency components will be recovered in a few iterations at first, while high frequency components are recovered later. The random noise data are introduced to simulate the influence of the measurement error on the recovered flux. It will be shown that satisfactory results with noisy data can be obtained by stopping the iteration process after an optimal number of steps.

2.2 Application of optimization method

The technique of optimization by the conjugate gradient method requires us to solve a sensitivity problem and an adjoint problem.

The conjugate gradient method has some principal advantages, which are as follows below:

(1) The speed of convergence is faster in solving unconstrained optimal problems (quadratic convergence) ;

(2) The performance about the uniqueness of the optimum in the considered domain is

better.

(3) This optimal method is relatively simple and it is easy to calculate.

With the optimization concept, the inverse conduction problem described above may be transformed into the following minimization problem.

Given the thermal physical properties, initial condition and a set of temperature measurements T_m at R_m, find the boundary heat flux $q(t)$ on S $(x=0)$ that minimizes the objective functional [3].

$$
\begin{aligned}
E &= \frac{1}{2}\|T - T_m\|^2 \\
&= \frac{1}{2}\langle T - T_m | T - T_m \rangle \\
&= \frac{1}{2}\int_0^{t_f} [T - T_m]^2 \, dt
\end{aligned}
\tag{2.1}
$$

where, E is the square error between the predicted temperature T, (corresponding to q) and the desired temperature T_m. The initial system is at an initial temperature T_i . At t > 0, the boundary of the surface S is subjected to a flux q .

According to Eq.(2.1), it is understood that there will be one sensor. If several sensors are considered, the functional becomes the sum of individual contributions like Eq.(2.1) at each location.

The minimization problem above consists of constructing a sequence

$q^1, q^2, q^3, \cdots, q^k, q^{k+1}, \cdots$

Such that

$$E^{k+1} < E^k$$

This can be done by the conjugate gradient method which gives

$$q^{k+1} = q^k + \alpha^k \cdot p^k$$

where, q^k is the value of minimizing the object function, α^k is the step size and p^k is the conjugate search direction.

Its true optimum solution will strongly depend on the ill-posedness of problem as well as the initial guess of its solution.

When a priori information is available such that $q\ (t)$ can be expressed in terms of a set of basic functions $\{f_i, i = 1,2,\cdots,N\ \}$, the problem is that of the minimization in a finite N-dimensional function space. The gradient of $E(q\ )$ can be determined in a rather straightforward manner. When no a priori information is available on $q\ (t)$, one has to deal with a completely unknown function, i.e., with an optimization problem in an infinite dimensional function space. Then, the minimizing an object function $E(q\ )$ requires the solutions of the adjoint problem and the sensitivity problem described in the following chapters.

To minimize E, it is necessary to determine its gradient in the infinite - dimensional space of q , if we do not possess any a priori information about

this unknown function.

One step of the algorithm [48], in particular, is rightly devoted to the computation of gradient. When some a priori information is assumed for the flux, such as a linear combination of n known functions, then the minimization of objective function is done over all possible coefficients of the combination. In this case, the parameter space over which minimization occurs is n-dimensional, and the gradient of E is nothing but the usual gradient in R^n. When no a priori information is available on $q(t)$, minimization must be implemented over an infinite-dimensional function space. In this case, the gradient of E and step size α can be obtained from solution of the adjoint and sensitivity problems.

2.3 Equation of sensitivity

To achieve the solutions, we have to define the sensitivity temperature. The definition of sensitivity temperature $\tilde{T}$ is that $\tilde{T}$ is the directional derivative of T at q in the direction Δq i.e.

$$\tilde{T} = \lim_{\varepsilon \to 0} \frac{f(q + \varepsilon \Delta q) - f(q)}{\varepsilon} \tag{2.2}$$

According to the definition of the temperature sensitivity $\tilde{T}$, we can take the directional derivative of the governing equation:

$$\frac{\partial T}{\partial t} = \nabla^2 T \tag{2.1}$$

then we obtain:

$$\frac{\partial \tilde{T}}{\partial t} = \nabla^2 \tilde{T} \tag{2.3}$$

and also satisfy:

the initial condition: $\tilde{T} = 0$ (2.4)

consisting with Eq.(1.4), then

the boundary condition: $\frac{\partial \tilde{T}}{\partial x}\Big|_{x=0} = \Delta q(t)$ (2.5)

the adiabatic conditions on the horizontal walls and $\tilde{T} = 0$ at $x = L$.

According to the definition of sensitivity temperature $\tilde{T}$, we know that the sensitivity problem, with Δq as driving force, is linear just like the direct problem, and governed by the exact same equation.

2.4 Adjoint equation

When minimization occurs over an infinite-dimensional space, there is no simple way to determine the gradient of functional E from its definition. It may be found instead from the solution of a set of adjoint equations. Although the method to obtain the latter is well known for inverse heat conduction problems, it has been only very recently developed for inverse natural convection problems.

Now, the derivation of the adjoint equation is shown in detail:

Suppose that a sensor is put in the middle of the field considered.

Set $T(x,y,t) = T(x,y,t,q^*)$, If $q^* \neq q$ (real value), then we get $T - T_m \neq 0$ (error) at

the sensor position. This leads us to the definition of the error in a more formal way. According to the definition:

$$E(q) = \frac{1}{2}\int_0^{t_f} \left[T - T_m\right]^2 dt \tag{2.6}$$

On the other hand, from the definition of Eq(2.1), we readily deduce

$$D_{\Delta q}E(q) = \int_0^{t_f} (T - T_m)\tilde{T}\, dt \quad \text{at } \vec{r} = \vec{r}_m \tag{2.7}$$

which can be written as

$$D_{\Delta q}E(q) = \int_{t=0}^{t_f} \int_S (T - T_m)\tilde{T}\delta(\vec{r} - \vec{r}_m) \cdot dSdt = 0 \tag{2.8}$$

where, S is the solution domain, considered for the minimization of the function.

The constraint is

$$\frac{\partial \tilde{T}}{\partial t} = \nabla^2 \tilde{T} \tag{2.9a}$$

or :

$$\frac{\partial \tilde{T}}{\partial t} - \nabla^2 \tilde{T} = 0 \tag{2.9b}$$

E is minimum when Eq.(2.8) is satisfied, or, equivalently, when

$$\int_0^{t_f}\int_S (T-T_m)\tilde{T}\delta(\vec{r}-\vec{r}_m)\cdot dSdt+\int_0^{t_f}\int_S \bar{T}\left\{\frac{\partial\tilde{T}}{\partial t}-\nabla^2\tilde{T}\right\}\cdot dSdt=0 \tag{2.10}$$

where, $\bar{T}$ is an unknown multiplier

But we know, $\bar{T}\nabla^2\tilde{T}=\tilde{T}\nabla^2\bar{T}+\nabla\cdot(\bar{T}\nabla\tilde{T}-\tilde{T}\nabla\bar{T})$ (2.11)

So,

$$\int_0^{t_f}\int_S (T-T_m)\tilde{T}\delta(\vec{r}-\vec{r}_m)\cdot dSdt+$$

$$\int_0^{t_f}\int_S \left\{\bar{T}\frac{\partial\tilde{T}}{\partial t}-\tilde{T}\cdot\nabla^2\bar{T}-\nabla\cdot(\bar{T}\cdot\nabla\tilde{T}-\tilde{T}\cdot\nabla\bar{T})\right\}dSdt=0 \tag{2.12}$$

With the divergence theorem, Eq.(2.12) may be recast as

$$\int_0^{t_f}\int_S (T-T_m)\tilde{T}\delta(\vec{r}-\vec{r}_m)\cdot dSdt+\int_0^{t_f}\int_S \left\{\bar{T}\frac{\partial\tilde{T}}{\partial t}-\tilde{T}\cdot\nabla^2\bar{T}\right\}dSdt+$$

$$\int_0^{t_f}\int_C (-\bar{T}\frac{\partial\tilde{T}}{\partial n}+\tilde{T}\frac{\partial\bar{T}}{\partial n})dldt=0 \tag{2.13}$$

On the C contour, it follows from Eq.(1.3), Eq.(1.4) and Eq.(1.5),

$\tilde{T}=0$ where T is known (2.14)

$$\frac{\partial \tilde{T}}{\partial n} = 0 \text{ where } \frac{\partial T}{\partial n} \text{ is known} \tag{2.15}$$

$$\frac{\partial \tilde{T}}{\partial n} = -\Delta q \text{ on } Ca \text{ (active boundary)} \tag{2.16}$$

We require $\bar{T}$ to satisfy the same conditions as $\tilde{T}$, with

$$\frac{\partial \bar{T}}{\partial n} = 0 \text{ on } C\,a \tag{2.17}$$

So, Eq.(2.13) becomes

$$\int_0^{t_f} \int_S (T - T_m)\tilde{T}\delta(\vec{r} - \vec{r}_m) \cdot dSdt + \int_0^{t_f} \int_S \left\{ \bar{T}\frac{\partial \tilde{T}}{\partial t} - \tilde{T} \cdot \nabla^2 \bar{T} \right\} dSdt +$$

$$\int_0^{t_f} \int_{Ca} \bar{T}\Delta q dl dt = 0 \tag{2.18}$$

But,

$$\int_0^{t_f} \int_S \bar{T}\frac{\partial \tilde{T}}{\partial t} dSdt = \int_0^{t_f} \frac{d}{dt} \int_S \bar{T}\tilde{T} dSdt - \int_0^{t_f} \int_S \tilde{T}\frac{\partial \bar{T}}{\partial t} dSdt -$$

$$\int_0^{t_f} \int_C \vec{V} \cdot \vec{n}\bar{T}\tilde{T} dl dt \tag{2.19}$$

Due to the fact that $\tilde{T} = 0$ on the moving boundary C, the third integral on the right-hand side vanishes,

We get

$$\int_0^{t_f} \overline{T}\frac{\partial \tilde{T}}{\partial t}dt = \overline{T}\cdot\tilde{T}\Big|_{t_f} - \overline{T}\cdot\tilde{T}\Big|_0 - \int_0^{t_f} \tilde{T}\frac{\partial \overline{T}}{\partial t}dt \tag{2.20}$$

We require

$$\overline{T} = 0 \text{ at } t = t_f \tag{2.21}$$

It is the initial condition for $\overline{T}$. Eq.(2.18) is then

$$\int_0^{t_f}\int_S \{-\frac{\partial \overline{T}}{\partial t} - \nabla^2\overline{T} + (T - T_m)\delta(\vec{r} - \vec{r}_m)\}\tilde{T}\cdot dSdt +$$

$$\int_0^{t_f}\int_{Ca} \overline{T}\Delta q dldt = 0 \tag{2.22}$$

We now require that

$$\frac{\partial \overline{T}}{\partial t} + \nabla^2\overline{T} = (T - T_m)\delta(\vec{r} - \vec{r}_m) \tag{2.23}$$

This is the adjoint equation.

The gradient of E, ∇E is related to the directional derivative of E, $D_{\Delta q_0}E(q)$, by the formal relationship:

$$D_{\Delta q}E(q) = \int_{t=0}^{t_f}\int_{Ca} \nabla E\Delta q\ dldt \tag{2.24}$$

On the other hand, we have just shown that

$$D_{\Delta q}E(q) = \int_{t=0}^{t_b} \int_{Ca} \overline{T}\Delta q dl dt \tag{2.25}$$

We therefore have

$$\nabla E = \overline{T}\,|_{Ca} \tag{2.26}$$

i.e. the gradient of the object function is equal to the adjoint temperature on the surface S.

Hence, E is minimum if $\nabla E = \bar{T}$ on active boundary where

$$\frac{\partial \overline{T}}{\partial t} + \nabla^2 \bar{T} = (T - T_m)\delta(\vec{r} - \vec{r}_m) \tag{2.27}$$

2.5 Minimization algorithm

It is clear by now that the minimization procedure that will lead to a solution for the inverse heat conduction problem involves the solution of three coupled equations with their own initial and boundary conditions. One has therefore to solve the direct, sensitivity, and adjoint problems at every step of the sequence of approximations for the minimizer.

The sensitivity and adjoint problems developed in the previous sections provide the necessary information for solving the infinite dimensional optimization problem by the conjugate gradient method.

The equations may be solved by any appropriate method. A first-order implicit, control-volume approach based on the power-law scheme of Patankar was used here to perform the discretization. The discrete equations were then solved by alternating line and column sweeps by the Thomas algorithm at each time step. More details are provided in Ref.[49].

For the adjoint equations, we first make the change of variable $\tau = t_f - t$ and start solving them for $\tau > 0$ with the initial condition at the physical time $t = t_f$. In other words, via this transformation, the adjoint problem is solved as an initial value problem in τ with positive diffusivity coefficient, which ensures numerical stability.

The main steps of this minimization technique are the following:

[1] Give initial conditions and choose initial guess q_0. Set iteration counter $k = 0$.

[2] Solve the direct problem with q^k to obtain T^k.

[3] Calculate the error between the given data and the calculated temperature field, i.e. $T^k - T_m$ at sensor's position.

[4] Solve the adjoint problem backward in time to obtain $\overline{T}^k$.

[5] Calculate the gradient $\nabla E^k = \overline{T}^k(0,t)$.

[6] Calculate the search direction p^k for Δq^k.

If $k = 0$, $p^k = -\nabla E^k$;

otherwise $p^k = -\nabla E^k + r^k p^{k-1}$

with $r^k = \dfrac{\left\langle \left(\nabla E^k - \nabla E^{k-1}\right), \nabla E^k \right\rangle}{\left\| \nabla E^{k-1} \right\|^2}$

[7] Solve the sensitivity equation with $\Delta q^{\,k} = p^k$ to obtain $\tilde{T}^k$ at the sensor position.

[8] Calculate the step size α^k for $\Delta q^{\,k} = \alpha^k p^k$.

$$\alpha^k = -\frac{\left\langle \nabla E^k, p^k \right\rangle}{\left\| \tilde{T}^k (x_m, t) \right\|^2}$$

[9] Update $q^{\,k+1} = q^{\,k} + \alpha^k p^k$.

[10] Set $k = k+1$, go back to step 2, repeat until convergence criterion $E^k < \varepsilon$ is satisfied.

[11] Output the results.

CHAPTER III

NUMERICAL IMPLEMENTATION

Focusing attention on the field values at the grid points, we have replaced the continuous information contained in the exact solution of the differential equation with discrete values. It is this systematic discretization of space and of the dependent variables that makes it possible to replace the governing differential equations with simple algebraic equations which can be solved with relative ease [48].

For a given differential equation, the required discretization equations can be derived in many ways. For example, Taylor-Series Formulation, Variational Formulation, Method of weighted Residuals, Control-Volume Formulation and so on. We shall adopt the control volume approach in this thesis.

The most attractive feature of the control-volume formulation is that the resulting solution would imply that the *integral* conservation of quantities such as mass, momentum, and energy is exactly satisfied over any group of control volumes and, of course, over the whole calculation domain. This characteristic exists for any number of grid points, not just in a limiting sense when the number of grid points becomes large. Thus, even the coarse-grid solution exhibits *exact* integral flux balances.

3.1 Discretization of the equations

For studying the inverse problem, the direct problem of heat conduction has to be discussed first and several cases are studied. The governing equation(1.2) is to be solved at the grid points of the mesh shown in Fig.3.1

$$\frac{\partial T}{\partial t} = \nabla^2 T \tag{1.2}$$

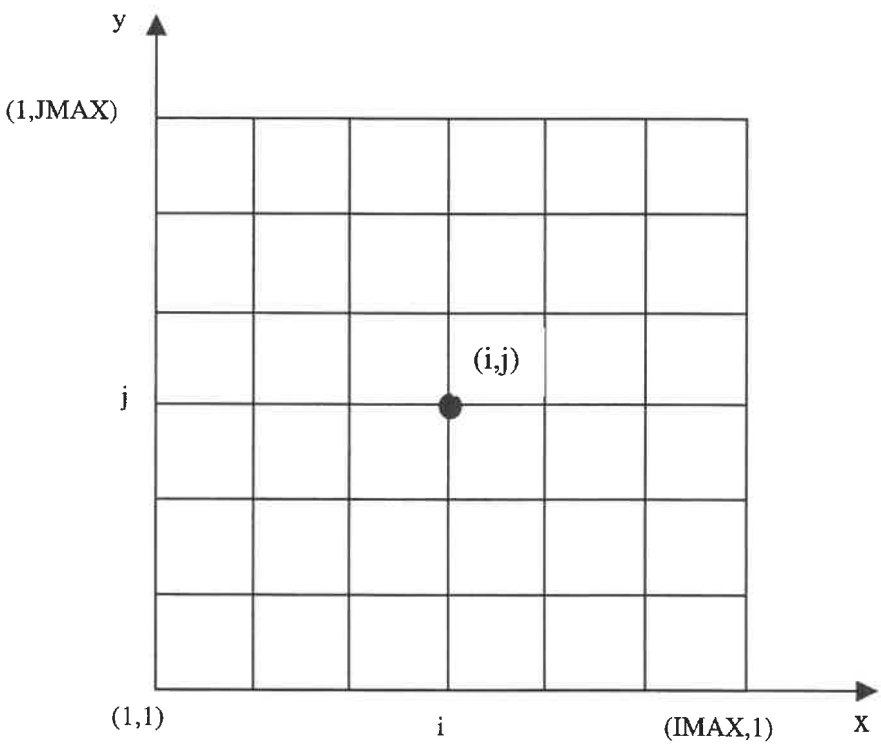

Figure 3.1 : Grid System of the Problem

There are various numerical techniques to perform discretization. Among these techniques, the finite difference approach is the most straightforward. But, some finite difference methods consume much time to calculate and produce wiggle solutions. Considering the governing equations and the boundary conditions, it is necessary for us to choose the appropriate numerical approach to solve these governing equations.

In the finite-difference approach, the domain is discretized so that the dependent variables are considered only at discrete points. For more universality, the two-dimensional grid system which is shown in Figure 3.1 are discussed in this chapter, Derivatives are approximated by differences, resulting in an algebraic representation of the partial differential equation(PDE). The nature of the resulting system of algebraic equations depends on the character of the problem posed by the original PDE.

A finite - difference method based on a control volume formation was used to obtain the numerical solution. The discretized equations were derived using a power-law interpolation scheme[49]for the spatial discretization and a standard first-order backward difference approximation for time derivatives. The discrete equations are then solved by alternating line and column sweeps by the Thomas algorithm at each time step.

The control volume of two-dimensional problem is shown in Figure 3.2, The control volume method is based on the integration of Eq.(1.2) over the control volume.

For any grid point P in the system, Eq. (1.2) has the discretized form

$$a_P T_P = a_E T_E + a_W T_W + a_N T_N + a_S T_S + b \tag{3.1}$$

where a_W, a_E, a_S, a_N, a_P and b are coefficients varying with the position of the node.

In the latter, P represents the current point under discussion. E, W, N, S, the neighbors of P at the east, west, north and the south, respectively and e, w, n, s are the mid points of the control volume interface, as we now show:

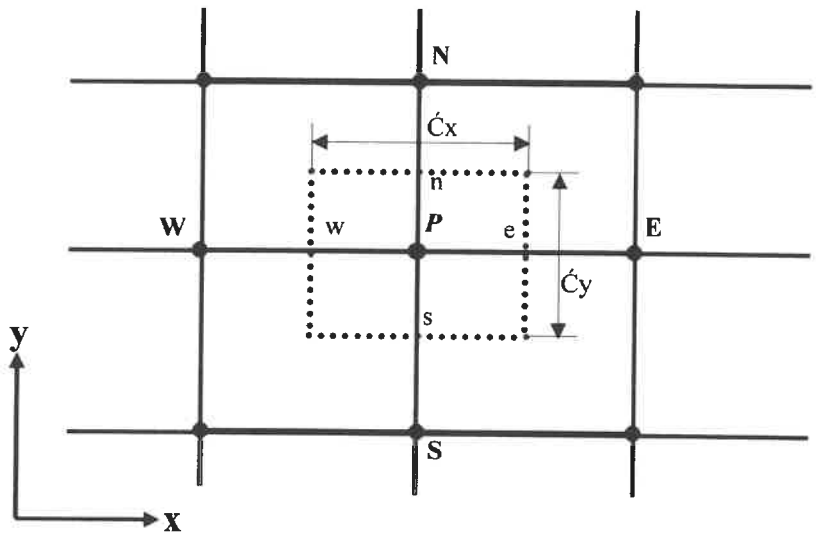

Figure 3.2 Control volume for internal node

For the convenience of the derivation, the definitions stated below are employed:

$$J_x = -\frac{\partial T}{\partial x} \tag{3.2}$$

$$J_y = -\frac{\partial T}{\partial y} \tag{3.3}$$

Then Eq.(1.2) becomes the following below:

$$\frac{\partial T}{\partial t} + \frac{\partial J_x}{\partial x} + \frac{\partial J_y}{\partial y} = 0 \tag{3.4}$$

Integrating the equation above, we can obtain easily with the divergence theorem

$$\frac{T_P - T_P^0}{\Delta t}\Delta x \Delta y + J_e \Delta y - J_w \Delta y + J_n \Delta x - J_s \Delta x = 0 \tag{3.5}$$

where

$$J_e = -\frac{(T_E - T_P)}{\Delta x} \tag{3.6}$$

$$J_w = -\frac{(T_P - T_W)}{\Delta x} \tag{3.7}$$

$$J_n = -\frac{(T_N - T_P)}{\Delta y} \tag{3.8}$$

$$J_s = -\frac{(T_P - T_S)}{\Delta y} \tag{3.9}$$

Substituting Eqs.(3.6-3.9) in Eq.(3.5) and rearranging the terms gives:

$$\frac{T_P - T_P^0}{\Delta t}\Delta x \Delta y - \frac{(T_E - T_P)\Delta y}{\Delta x} + \frac{(T_P - T_W)\Delta y}{\Delta x} - \frac{(T_N - T_P)\Delta x}{\Delta y} + \frac{(T_P - T_S)\Delta x}{\Delta y} = 0 \tag{3.10}$$

which can be stated in compact form as:

$$a_P T_P = a_E T_E + a_W T_W + a_N T_N + a_S T_S + b \tag{3.2}$$

where $a_P = \frac{\Delta x \Delta y}{\Delta t} + 2(\frac{\Delta x}{\Delta y} + \frac{\Delta y}{\Delta x})$

$$a_E = \frac{\Delta y}{\Delta x} = a_W$$

$$a_N = \frac{\Delta x}{\Delta y} = a_S$$

$$b = \frac{T_P^0 \Delta x \Delta y}{\Delta t}$$

are the finite difference coefficients.

For one-dimensional situations, $T_N = T_S = T_P$ and we have

$$a_P = \frac{\Delta^2 x}{\Delta t}$$

$$a_E = 1 = a_W$$

$$b = \frac{T_P^0 \Delta^2 x}{\Delta t}$$

3.2 Algorithm of solution

The organization chart of solution summarizes the process of the numerical solution of the direct problem equation. This algorithm is equally used in sensitivity problem and adjoint problem.

Flow Chart of Solution

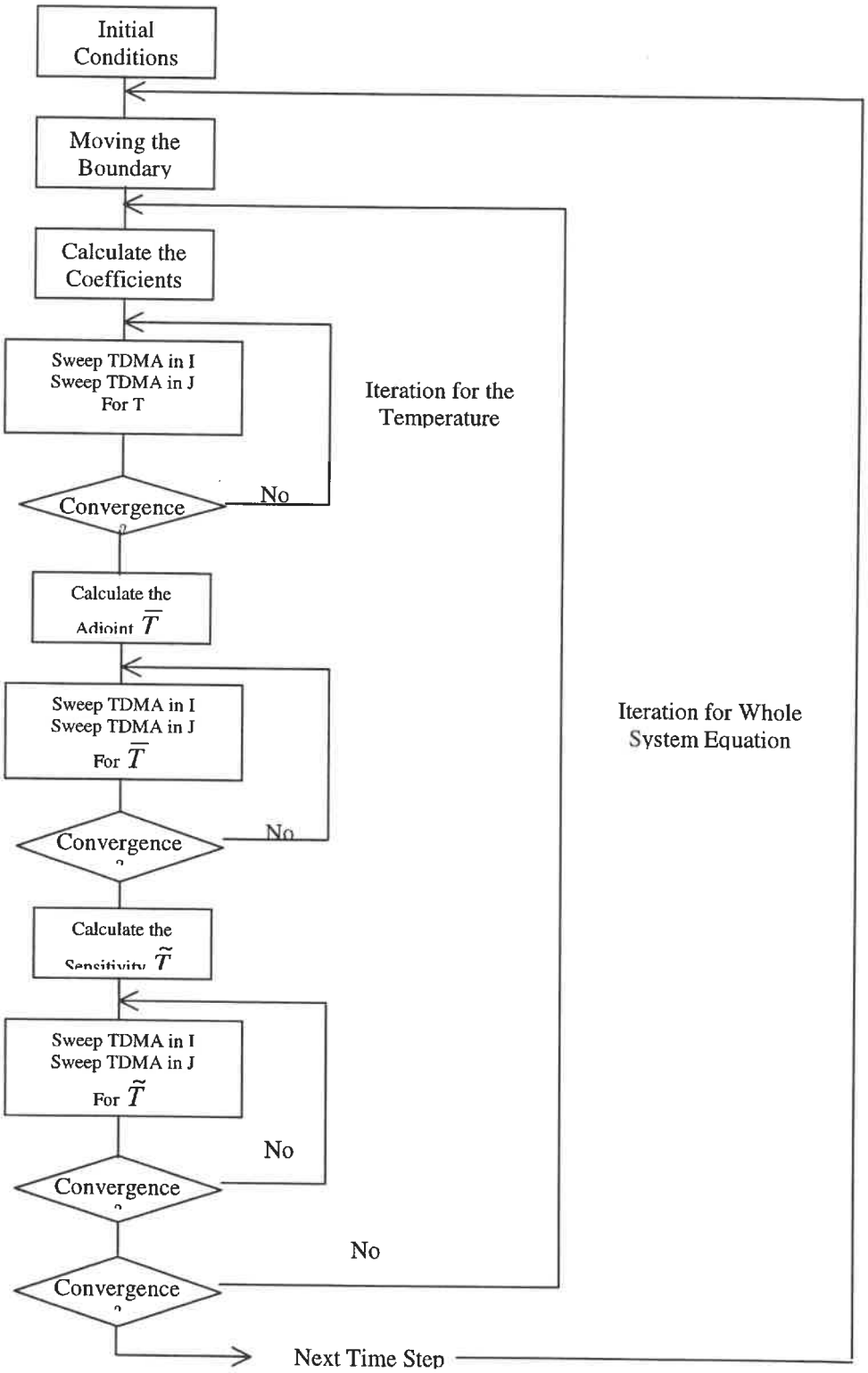

CHAPTER IV

RESULTS AND DISCUSSIONS

This chapter gives the solutions of direct and inverse problems for different conditions. The discussions for the two kinds of problems are provided.

4.1 Direct heat conduction problem

The solution of the direct problem is at the heart of the inverse problem solution procedure. Hence, direct conduction is discussed at first and some preliminary results will be obtained. Then, the solutions of the inverse problem are provided in the next section.

The figures given below are for 12 cases. (from Direct Solution Case $No.1$ to Direct Solution Case $No.9_2$). The different cases covered are given as follows below.

Initial condition (at $t = 0.0$)

$$L = L_0 = 1$$
$$T = T_0 = 0$$

The boundary conditions correspond to incoming heat fluxes in the domain, like in a situation where one would seek to induce melting of a substance.

$$q = q(t) = -1, -t, -\sin(\omega t) \quad (\text{at } x = 0)$$
$$T = 0 \quad (\text{at } x = L)$$

The moving boundary velocity might be either prescribed as a constant or oscillating function (first and third cases) as proportional to the local flux normal to the boundary, (second case) as would occur in a melting problem.

$$V = \frac{dL}{dt} = 1.0$$

$$V = -\frac{dT}{dx}\Big|_{x=1.0}$$

$$V = \sin(\omega t)$$

In all the cases discussed in this chapter, the graph of temperature as a function of time is given at $x = 0$ and the graph of isotherms is provided at $t = 1.0$.

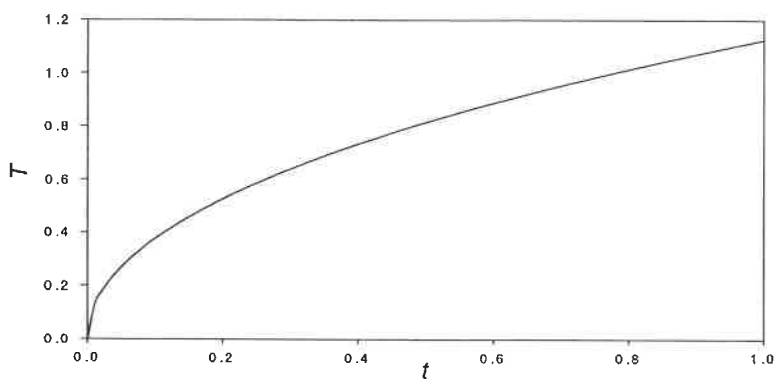

Figure 4.1 Direct Solution for Case 1 q=-1, V=1

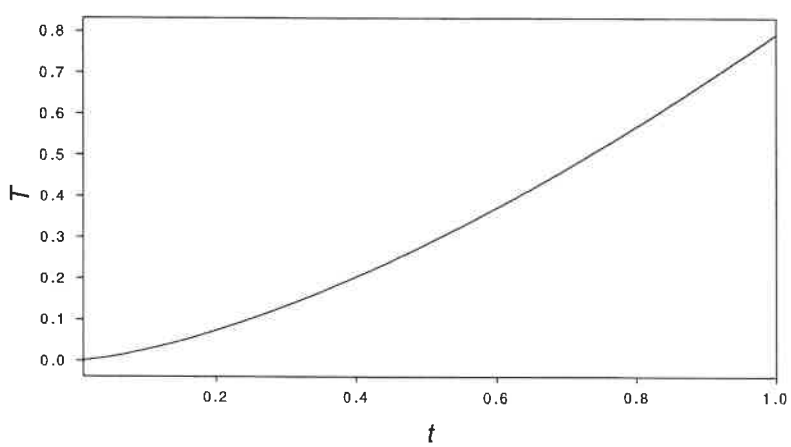

Figure 4.2: Direct Solution for Case 2 q=-t, V=1

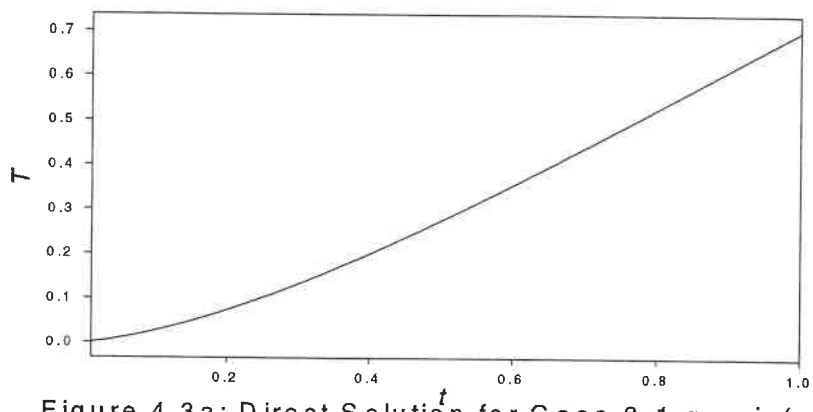

Figure 4.3a: Direct Solution for Case 3-1 q=-sin(wt) w=1, V=1

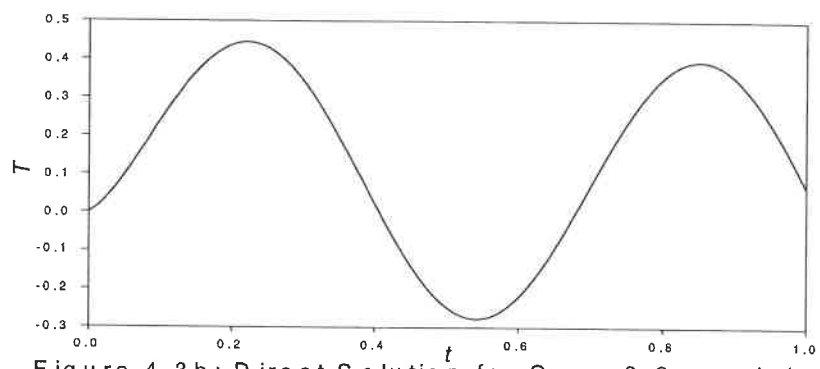

Figure 4.3b: Direct Solution for Case 3-2 q=-sin(wt) V=1, w=10

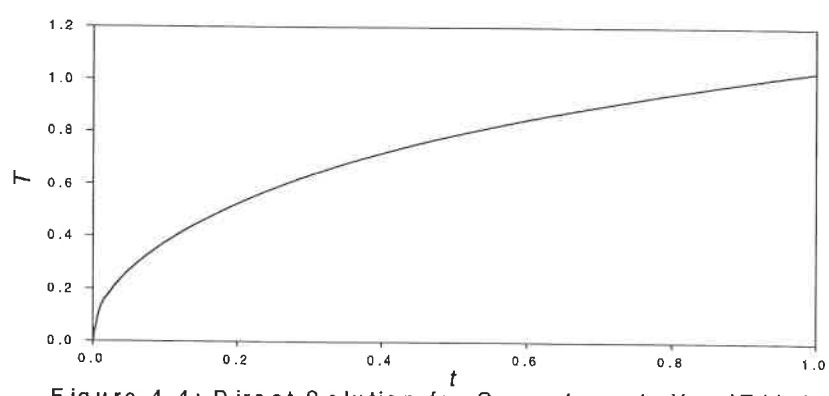

Figure 4.4: Direct Solution for Case 4 q=-1, V=-dT/dx|x=L

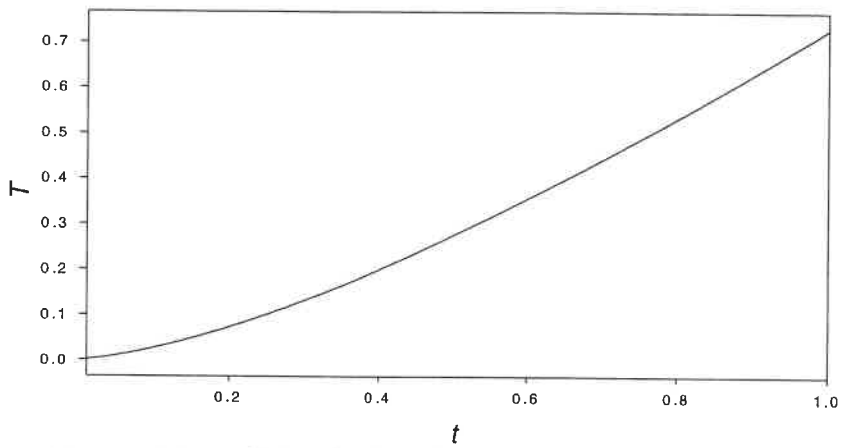

Figure 4.5: Direct Solution for Case 5 q=-t, V=-dT/dx|x=L

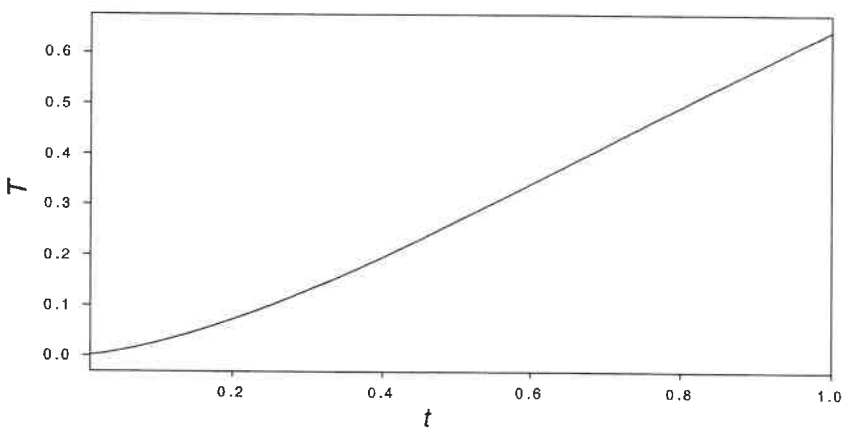

Figure 4.6a: Direct Solution for Case 6-1 q=-sin(wt)
V=-dT/dx|x=L, w=1

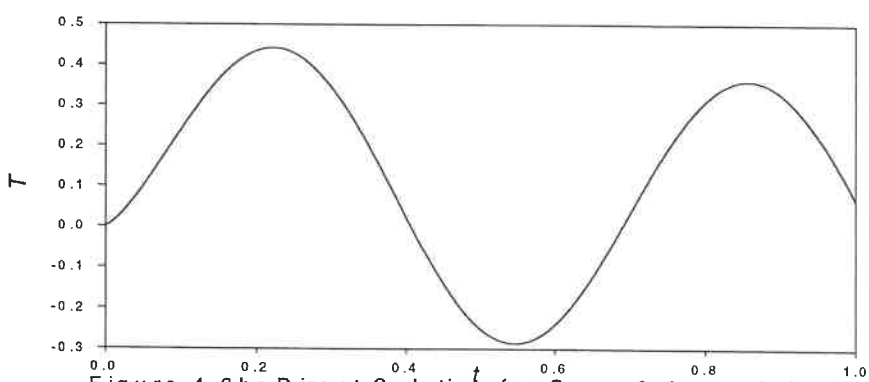

Figure 4.6b: Direct Solution for Case 6-2 q=-sin(wt)
V=-dT/dx|x=L, w=10

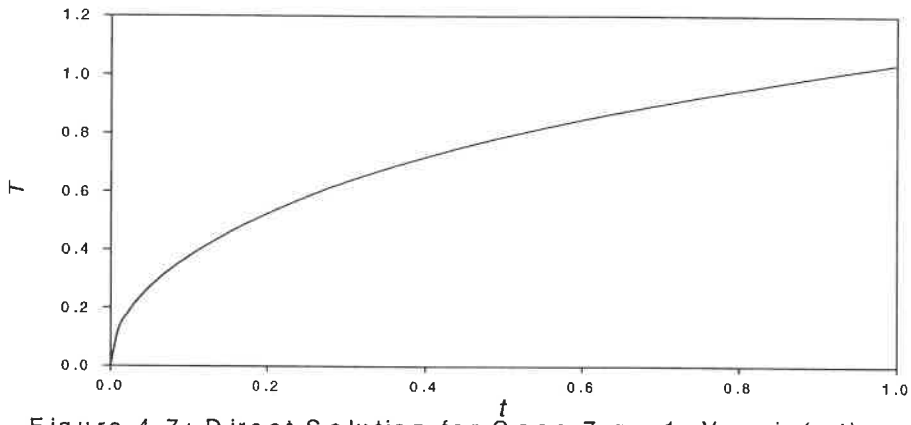

Figure 4.7: Direct Solution for Case 7 q=-1, V=-sin(wt), w=1

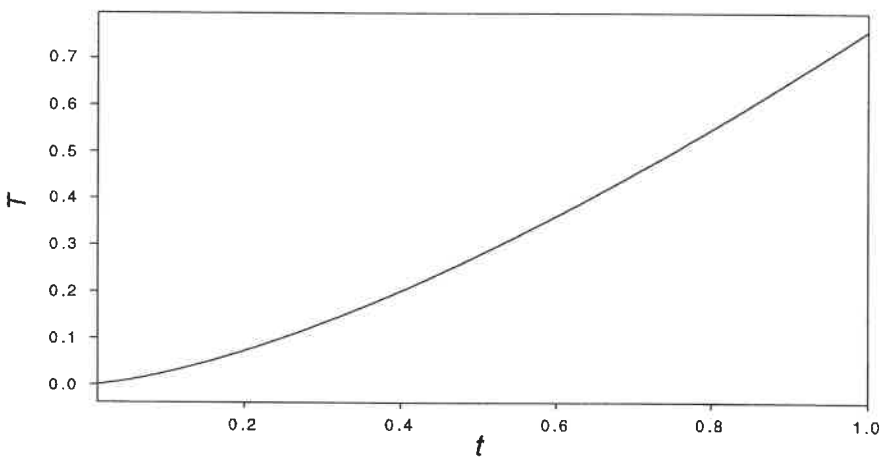

Figure 4.8: Direct Solution for Case 8 q=-t, V=sin(wt), w=1

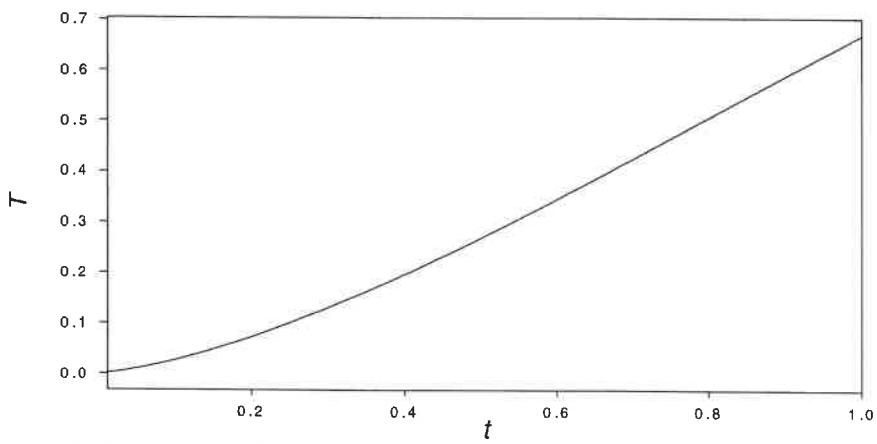

Figure 4.9a: Direct Solution for Case 9-1 q=-sin(wt)
V=sin(wt), w=1

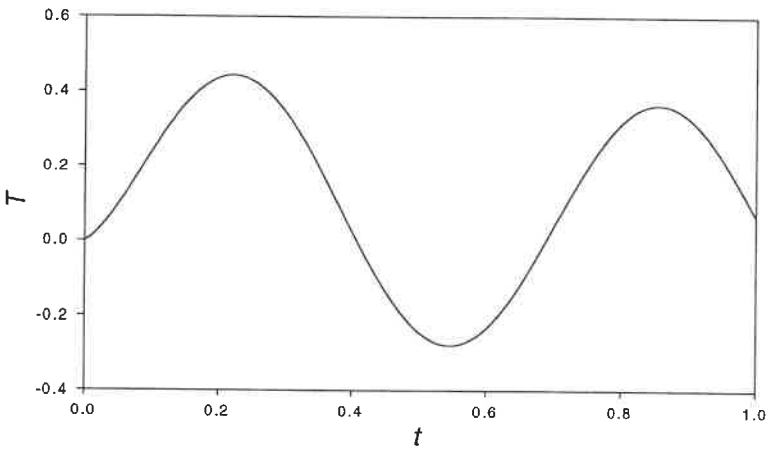

Figure 4.9b: Direct Solution for Case 9-2 q=-sin(w_1*t) V=sin(w_2*t), w_1=10, w_2=1

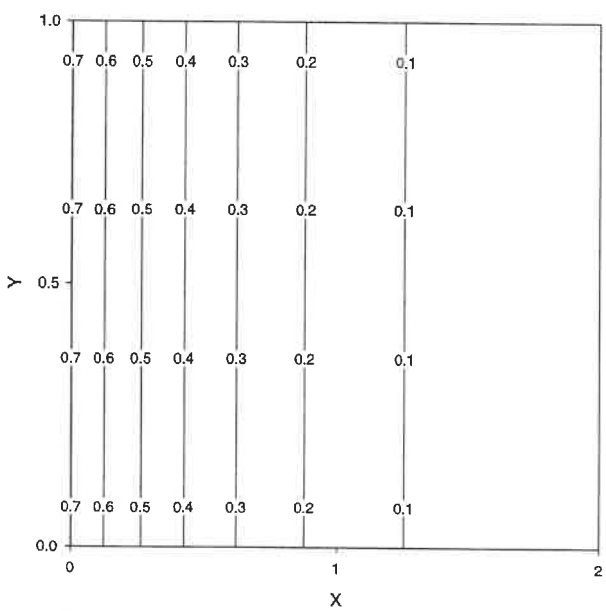

Figure 4.10: Isotherm Case 3-1 At t_f for q=-sin(wt) V=1, W=1

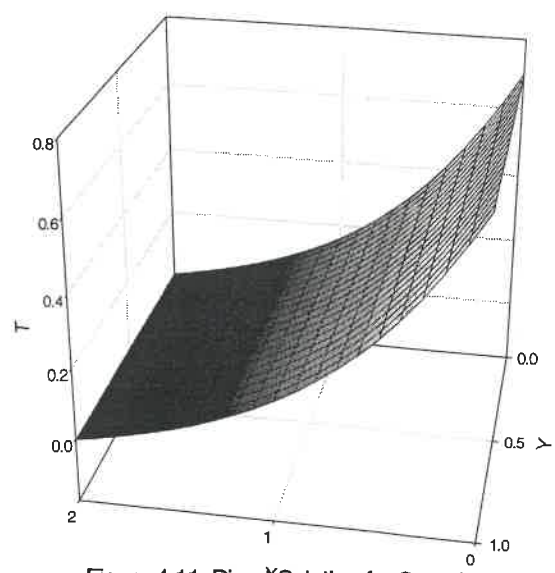

Figure 4.11: Direct Solution for Case 3-1 q=-sin(wt), V=1, w=1

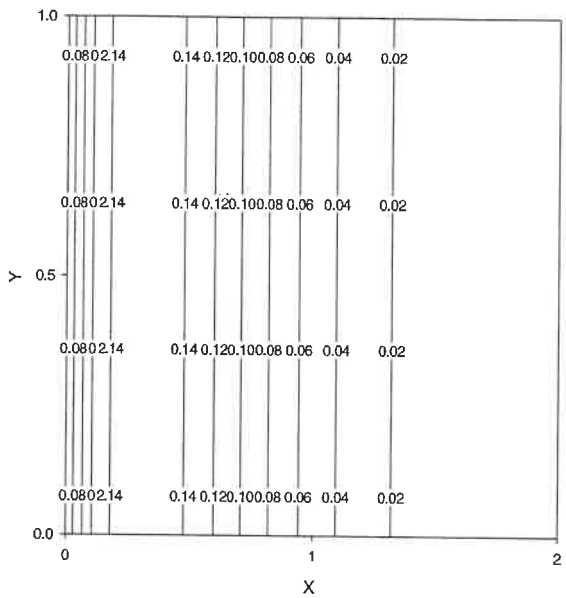

Figure 4.12: Isotherm for Case 3-2 At t_f for q=-sin(wt) V=1, w=10

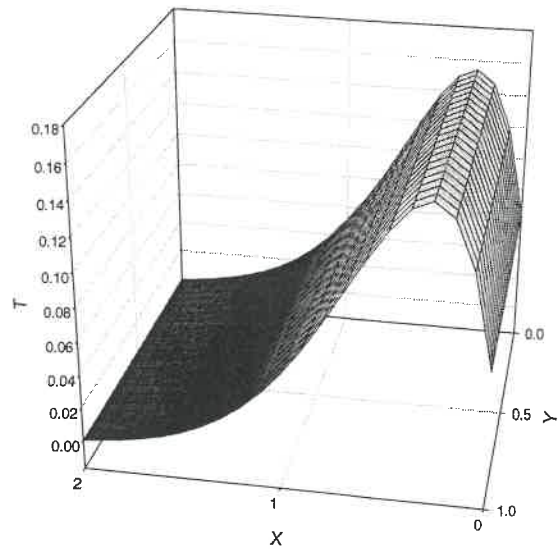

Figure 4.13: 3-D Temperature Field for Case 3-2 q=-sin(wt), V=1, W=10

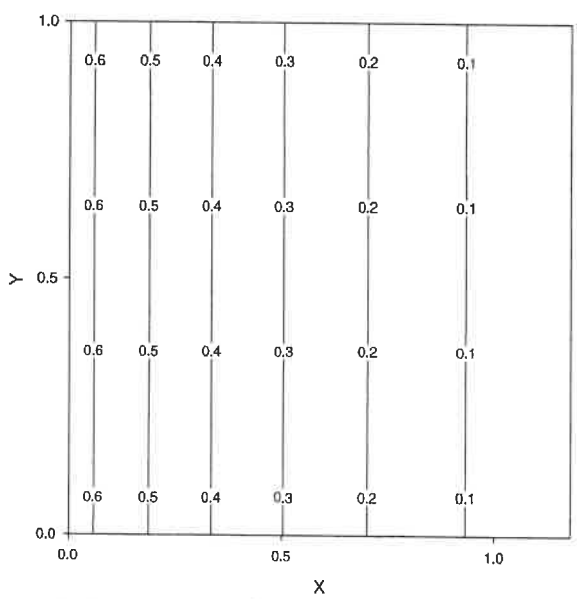

Figure 4.14: Isotherm Case 9-1 At t_f for q=-sin(w_1*t) V=sin(w_2*t), w_1=1, w_2=1

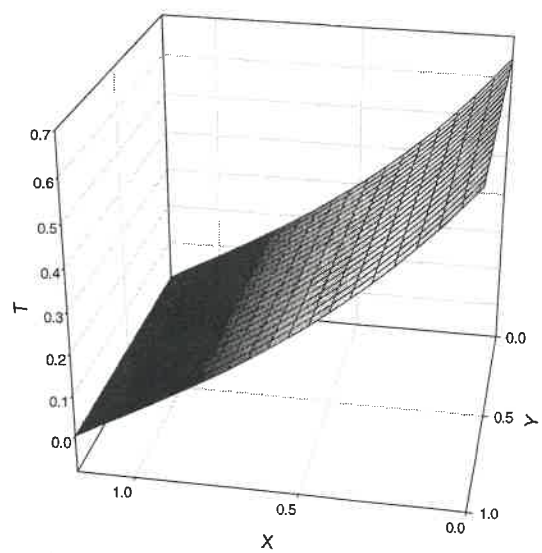

Figure 4.15: Direct Solution for Case 9-1 q=-sin(w_1*t) V=sin(w_2*t), w_1=1, w_2=1

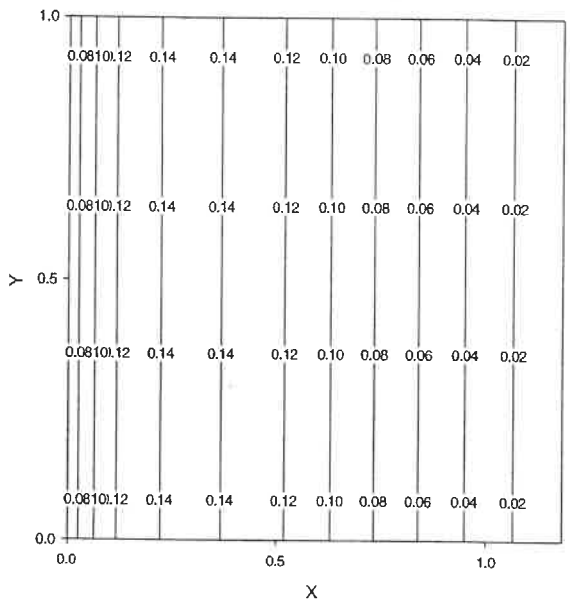

Figure 4.16 : Isotherm Case 9-2 At t_f for $q=-\sin(w_1*t)$ $V=\sin(w_2*t)$, $w_1=10$, $w_2=1$

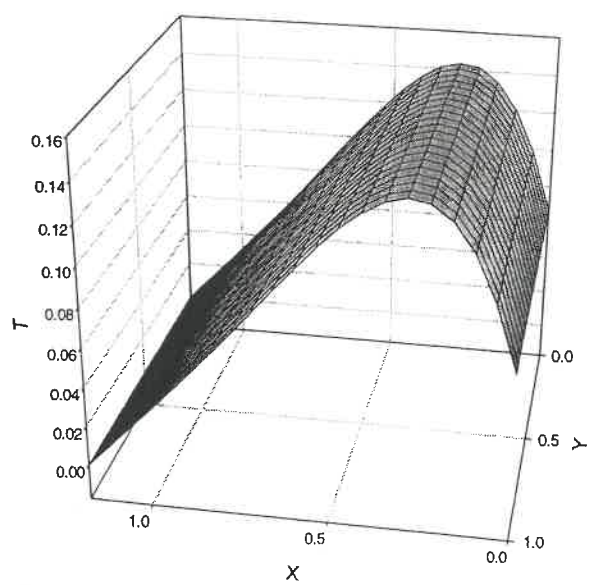

Figure 4.17: 3-D Temperature Field for Case 9-2 $q=-\sin(w_1*t)$ $V=\sin(w_2*t)$, $w_1=10$, $w_2=1$

From Direct Solution Case $No.1$ to Direct Solution Case $No.9_2$, we can conclude that

1. The temperature at $x = 0$ increases with time in all the different cases considered.

2. If the flux is periodic, the temperature is also varying (increasing and decreasing) with the same frequency, which is normal, since the equations are linear.

The isotherms for Case $No.3_1$, Case $No.3_2$, Case $No.9_1$ and Case $No.9_2$ are presented in Fig.4.10, Fig.4.12, Fig.4.14 and Fig.4.16.

From the graphs, the temperature is uniform in the Y direction. Thus, the solution varies only in the X direction as expected (A One-Dimensional problem is considered); and the temperature is decreasing with distance from $x = 0$ because the heat flux source is located at $x = 0$.

Also 3-D representations are provided for the temperature in the Case $No.3_1$, Case $No.3_2$, Case $No.9_1$ and Case $No.9_2$.

In this section, the figures above Fig.4.1 - Fig.4.17 prove that we can get satisfactory results in different kinds of situations. Hence, the direct problem code is adaptable to the situations considered here and valid for the cases considered, and the performance of convergence is good.

4.2 Inverse heat conduction problem

We now discuss the inverse solution for the cases under study presented earlier. The IHCP under consideration is depicted in Fig.4.18 - Fig. 4.99.

(1) Case *No.*1

For this situation (From Fig.4.18 to Fig.4.24), the flux is constant and the velocity is also a prescribed constant.

$$q = q(t) = -1$$

$$V = 1.0$$

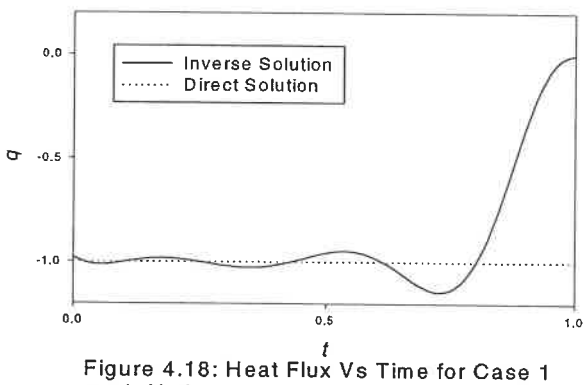

Figure 4.18: Heat Flux Vs Time for Case 1 q=-1, V=1

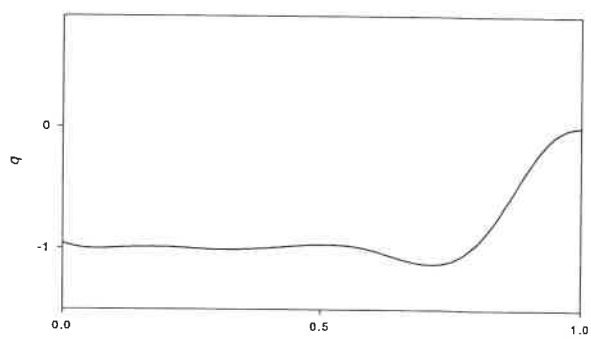

Figure 4.19: Inverse Solution of Heat Flux for Case 1 q=-1, V=1 and Sigma=0.001

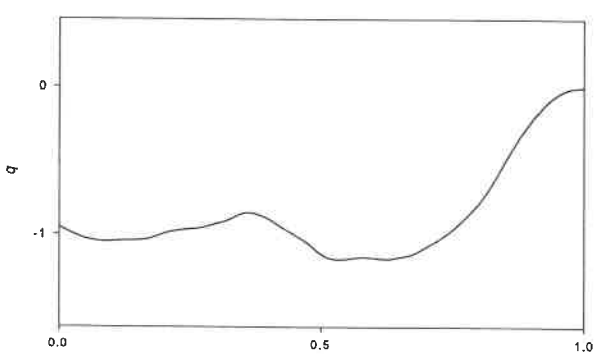

Figure 4.20: Inverse Solution of Heat Flux for Case 1 q=-1,V=1 and Sigama=0.04

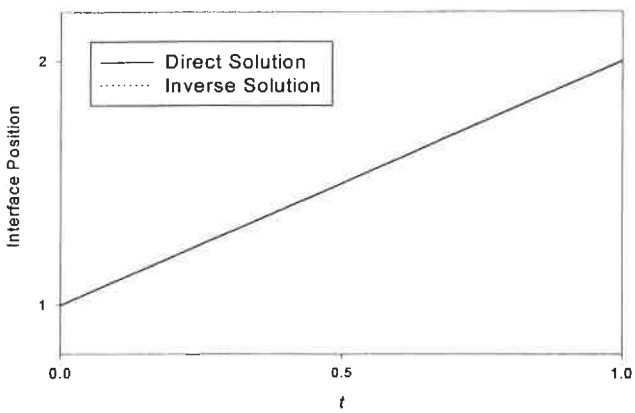

Figure 4.21: Interface Position Vs Time for Case 1 q=-1, V=1

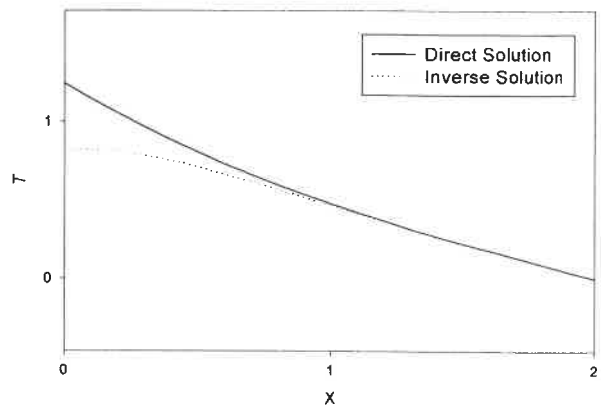

Figure 4.22: Contrast Between Direct Solution and Inverse Solution of Temperature for Case1 q=-1, V=1 at $t=t_f$

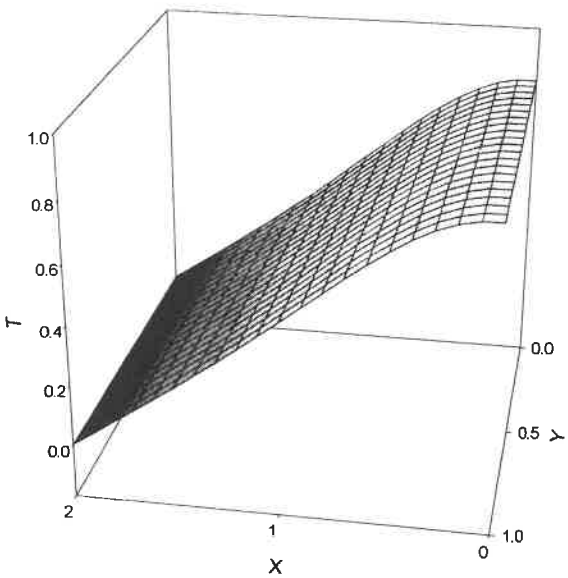

Figure 4.23: 3-D Inverse Solution for Case 1 q=-1, V=1

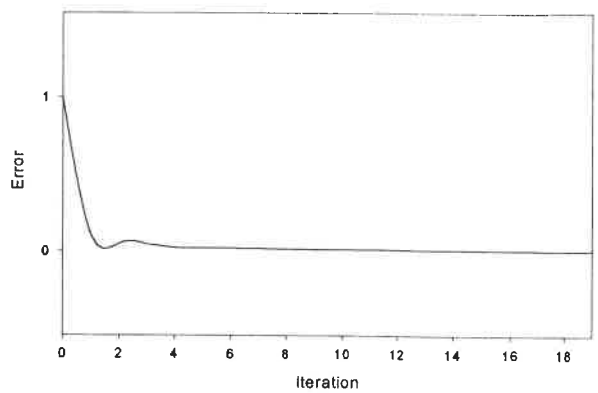

Figure 4.24: Error Evolution for Case 1 q=-1, V=1

According to Fig.4.18, the original flux can be recovered. At the beginning, the inverse solution is very close to the direct solution (real value), but near the end at t_f, the discrepancy is increasing. Especially, the discrepancy is maximal at $t = 1$ because the flux$(q) \neq 0$ at $t = 1$ but the adjoint temperature is always equal to zero.

The recovered interface position is perfect, because it is independent of the flux and temperature. It is shown in Fig.4.21.

From Fig. 4.19 to Fig. 4.24 (Except Fig.4.21), we can get some conclusion from the results.

a. The inverse temperature is recovered well at t_f except in the vicinity of the point $x = 0$.

b. When the number of iterations is less than 3, the error is very big. But when the number of iteration is greater than 4, the error is very small.

c. when noisy data is considered, the simulations for a standard deviation $\sigma = 0.001$ is better than for a deviation $\sigma = 0.04$.

(2) Case *No*.2

For this case (From Fig.4.25 to Fig.4.31), the flux is linear in time and the velocity remains prescribed at the same constant value.

$$q = q(t) = -t$$

$$V = 1.0$$

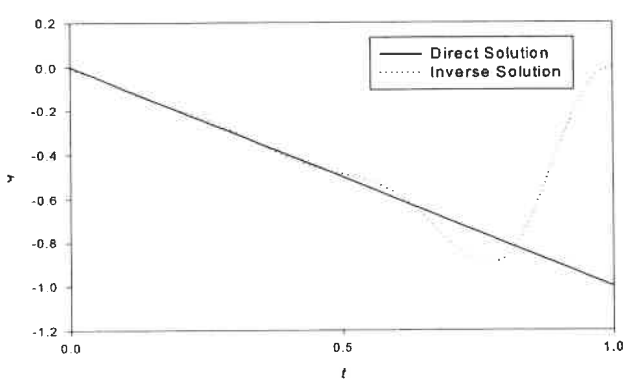

Figure 4.25: Heat Flux Vs Time for Case 2 q=-t, V=1

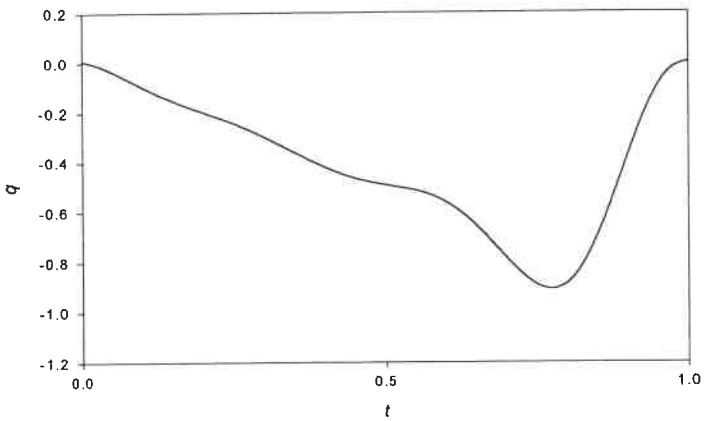

Figure 4.26: Inverse Solution of Heat Flux for case 2 q=-t V=1, Sigma=0.001

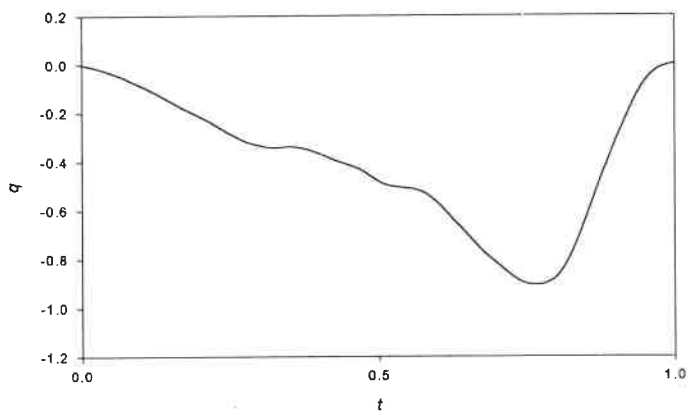

Figure 4.27: Inverse Solution of Heat Flux for Case 2 q=-t V=1, Sigma=0.04

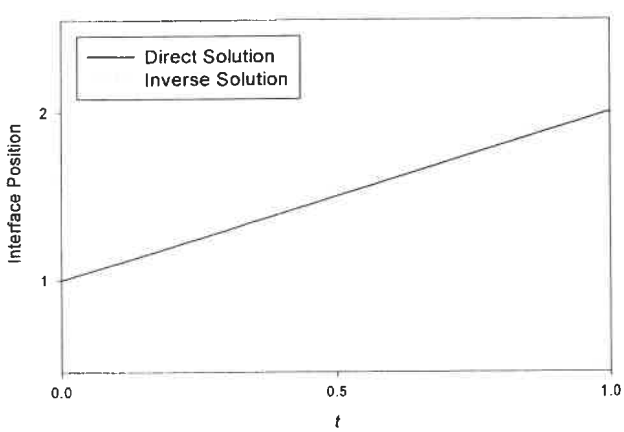

Figure 4.28: Interface Position Vs Time for Case 2 q=-t, V=1

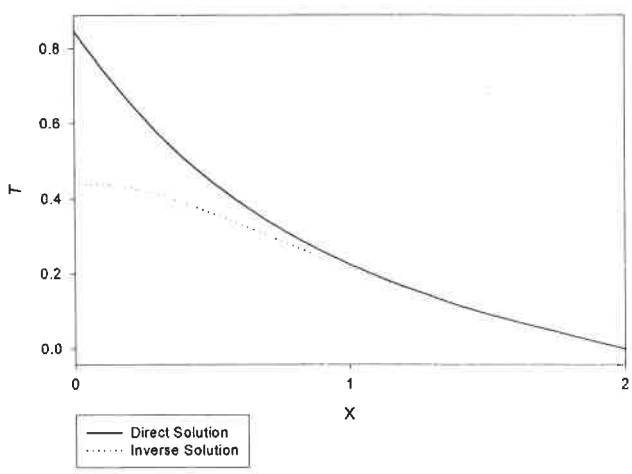

Figure 4.29: Contrast Between Direct Solution and Inverse Solution of Temperature for Case 2 q=-t, V=1 at $t=t_f$

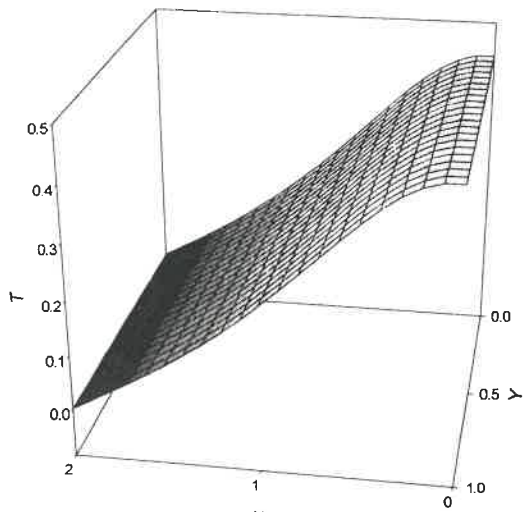

Figure 4.30: 3-D Inverse Solution for Case 2 q=-t, V=1

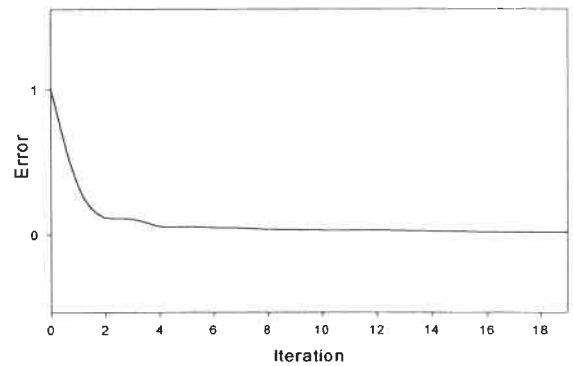

Figure 4.31: Error Evolution for Case 2 q=-t, V=1

The results as a whole are similar to those for the Case $No.1$. The noisy data influence (for $\sigma = 0.001$ and $\sigma = 0.04$) on the recovered flux is the same as (2) Case No.2.

(3) Case $No.3_1$

For this case (From Fig.4.32 to Fig.4.38), the flux is periodic and the velocity is constant as follows.

$$q = q(t) = -\sin(\omega\pi t) \quad (\omega = 1)$$

$$V = 1.0$$

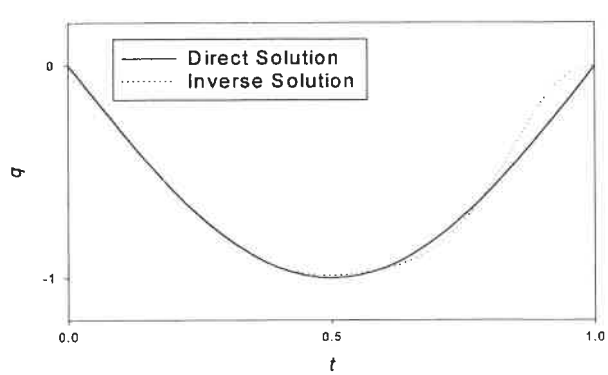

Figure 4.32: Heat Flux Vs Time for Case 3-1 q=-sin(w*PI*t), V=1, w=1

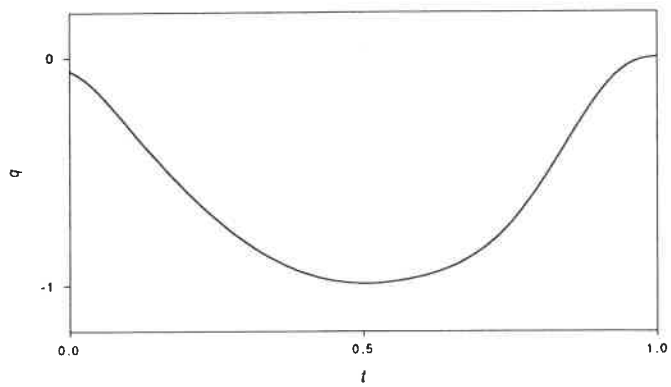

Figure 4.33: Inverse Solution of Heat Flux for Case 3-1
q=-sin(w*PI*t), V=1, w=1, Sigma=0.001

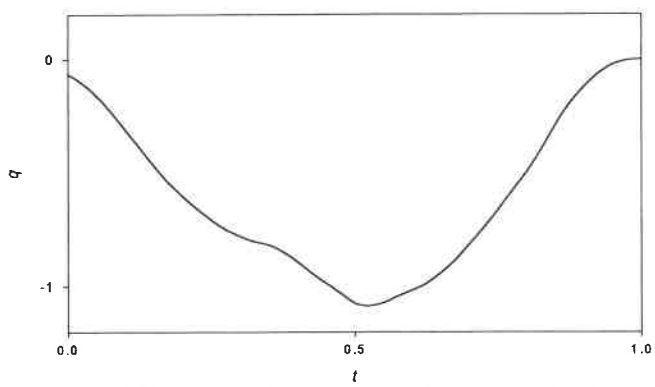

Figure 4.34: Inverse Solution of Heat Flux for Case 3-1
q=-sin(w*PI*t), V=1, w=1, Sigma=0.04

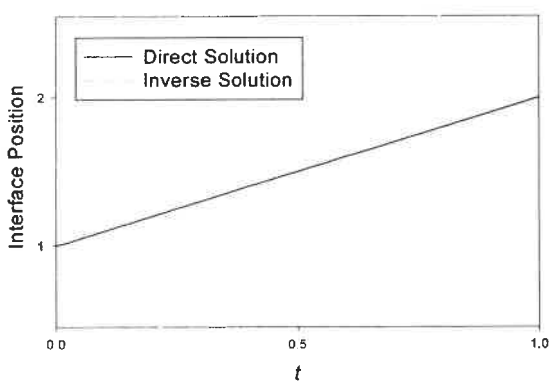

Figure 4.35: Interface Position Vs Time for Case 3-1
q=-sin(w*PI*t), V=1, w=1

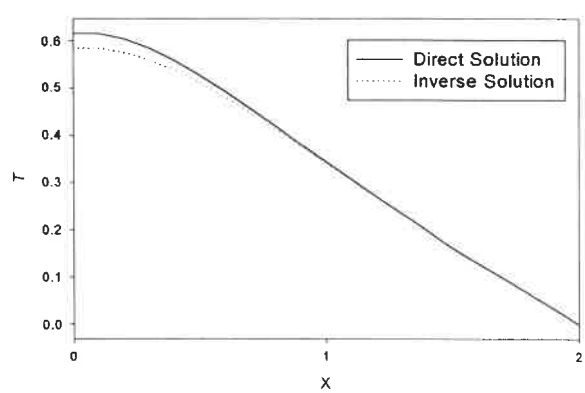

Figure 4.36: Contrast Between Direct Solution and Inverse Solution of Temperature for Case 3-1
q=-sin(w*PI*t), V=1,w=1

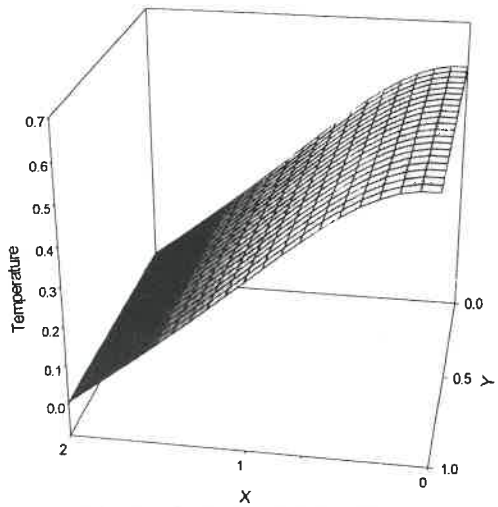

Figure 4.37: 3-D Inverse Solution for Case 3-1
q=-sin(w*PI*t), V=1, w=1

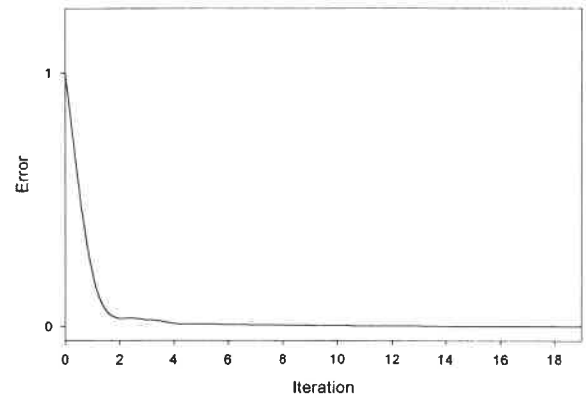

Figure 4.38: Error Evolution for Case 3-1
q=-sin(w*PI*t), V=1, w=1

The inverse flux is once again very well recovered, the temperature is also very close to the real value. Because at $t = 1.0$ where q is also equal to zero, the adjoint temperature is equal to zero, the inverse flux value is close to the real value near $t = 1.0$.

Fig.4.33 and Fig.4.34 give the heat flux for the noisy temperature data at the different standard deviation. These show the obvious influence of the different σ levels.

From Fig. 4.38, it is once more clear that the error is almost zero when the iteration number is greater than 4 or so.

(4) Case $No.3_2$

For this situation (From Fig.4.39 to Fig.4.45), the flux is periodic like before, but at a higher frequency,

$$q = q(t) = -\sin(\omega\pi t) \quad (\omega = 10)$$

$$V = 1.0$$

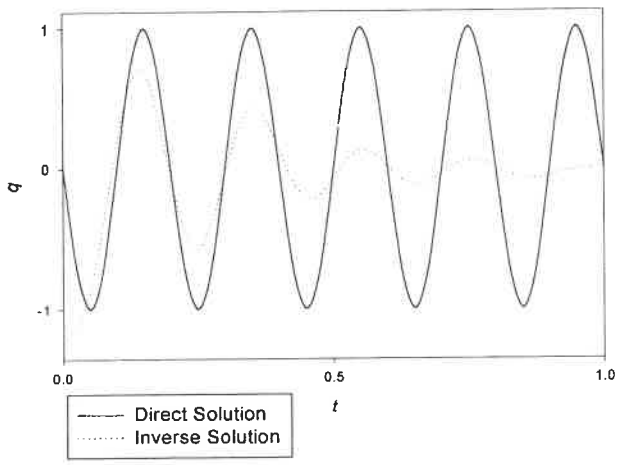

Figure 4.39: Heat Flux Vs Time Case 3-2 q=-sin(w*PI*t) V=1, w=10,Iteration=19

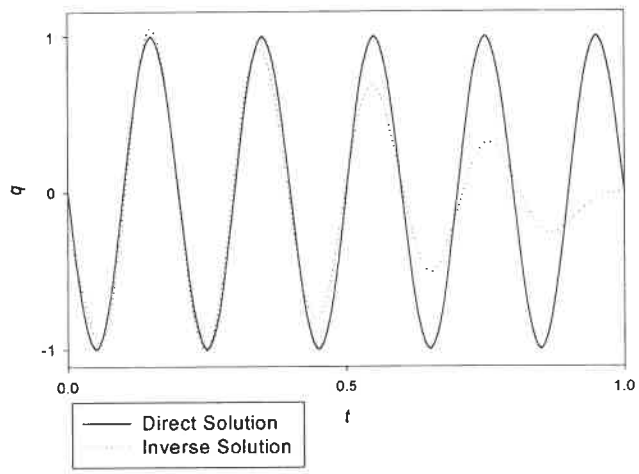

Figure 4.40: Heat Flux Vs Time for Case 3-2 q=-sin(w*PI*t) V=1, w=10 and Iteration=40

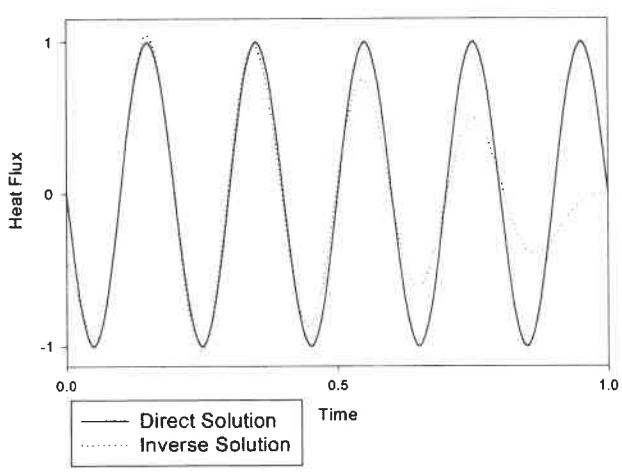

Figure 4.41: Heat Flux Vs Time for Case 3-2 q=-sin(w*PI*t) V=1, w=10 and Iteration=100

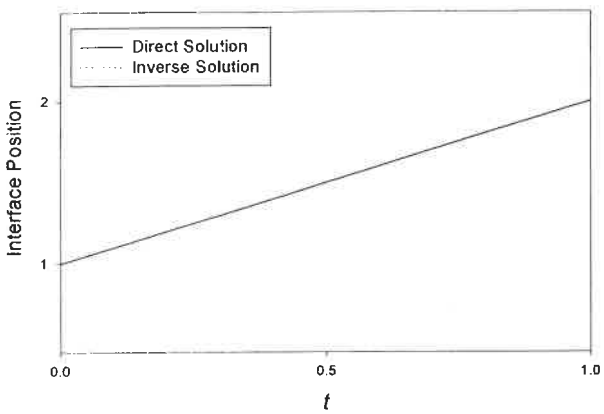

Figure 4.42: Interface Position Vs Time for Case 3-2 q=-sin(w*PI*t), V=1, w=10

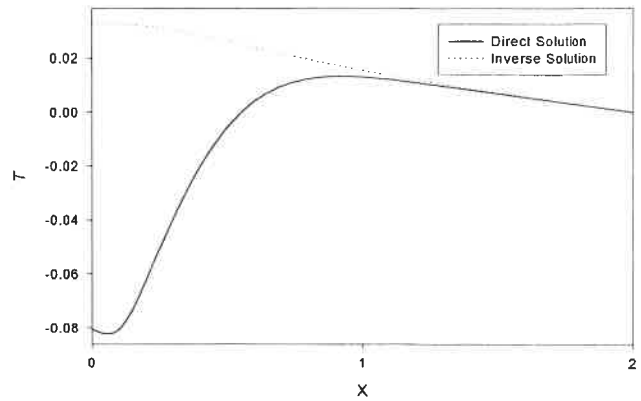

Figure 4.43: Contrast Between Direct Solution and Inverse Solution of Temperature for Case 3-2 q=-sin(w*PI*t) V=1, w=10

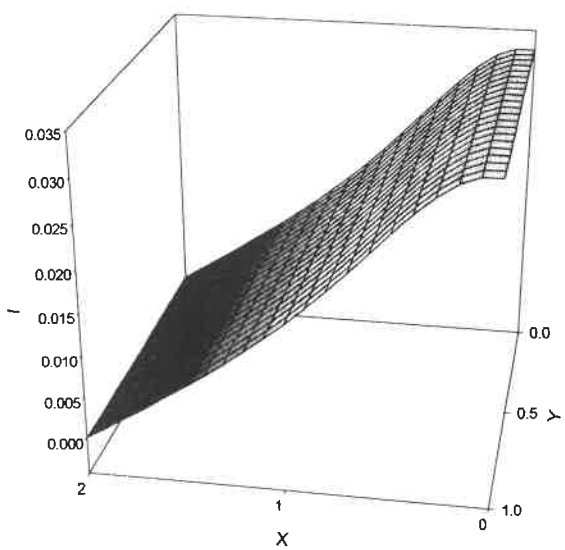

Figure 4.44: 3-D Inverse Solution for Case 3-2 q=-sin(w*PI*t), V=1, w=10

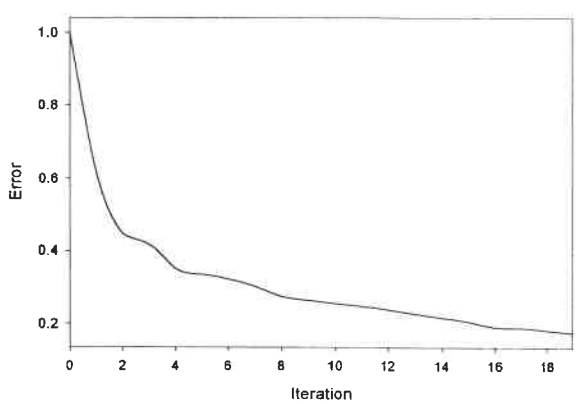

Figure 4.45: Error Evolution for Case 3-2 q=-sin(w*PI*t), V=1, w=10

For the higher frequency, the inverse solution is not like the one at lower frequency, for example Case $No.3-1$. From Fig.4.39, we can find that the greater discrepancy is found at the end of the time interval. And the inverse value is not accurate when approaching t=1.0. According to Fig.4.39, Fig.4.40 and Fig.4.41, the influence of the number of iteration is found to be very important. The best solution corresponds to 100 iterations. The worst one is for 19 iterations. So, we should increase the number of iterations when the inverse flux is of high frequency.

From Fig.4.45, we can find that the error is bigger than in the lower frequency situation.

(5) Case $No.4$

For this case (From Fig.4.46 to Fig.4.52), the heat flux is constant and the velocity is found from the local temperature gradient as follows below

$$q = q(t) = -1.0$$

$$V = -\frac{dT}{dx}\Big|_{x=l}$$

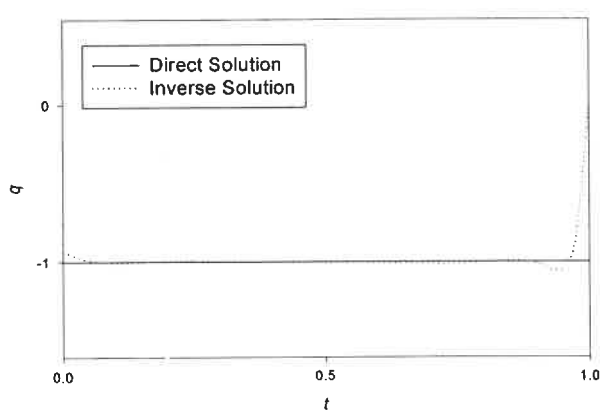

Figure 4.46: Heat Flux Vs Time for Case 4,q=-1
V=-dT/dx|x=L

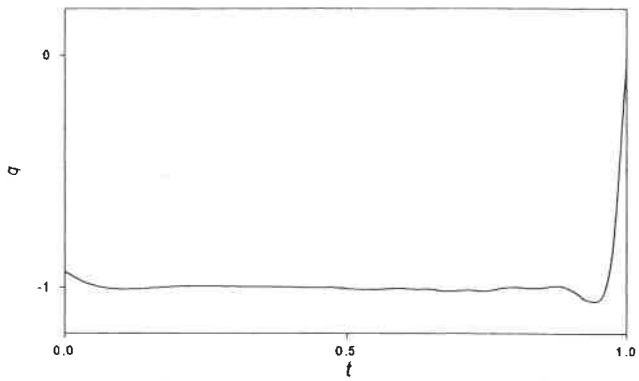

Figure 4.47: Inverse Solution of Heat Flux for Case 4 q=-1 V=-dT/dx|x=L, Sigma=0.001

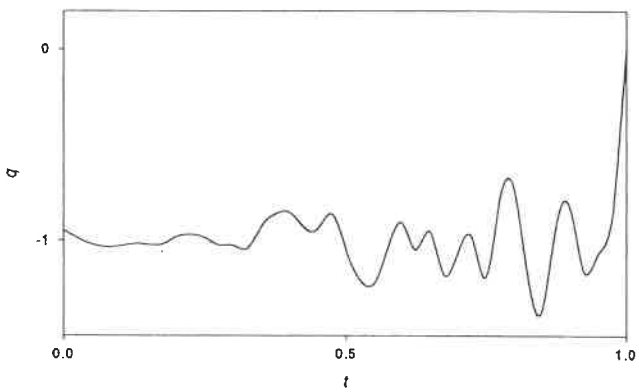

Figure 4.48 : Inverse Solution of Heat Flux for Case 4, q=-1 V=-dT/dx|x=L, Sigma=0.04

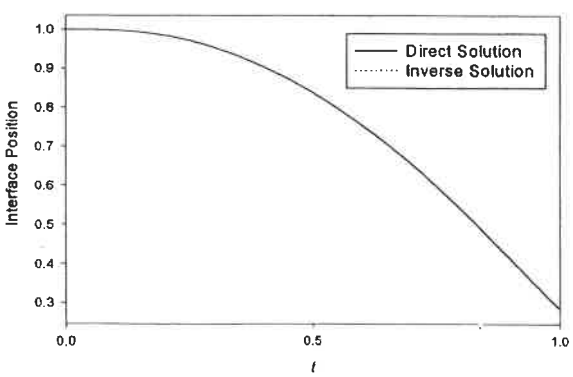

Figure 4.49: Interface Position Vs Time for Case 4 q=-1, V=-dT/dx|x=L

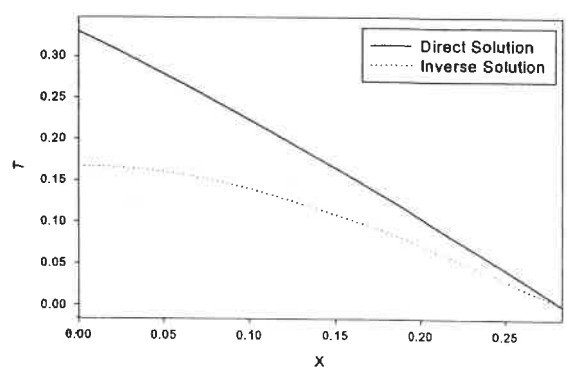

Figure 4.50 : Contrast Between Direct Solution and Inverse Solution of Temperature for Case 4 q=-1 V=-dT/dx|x=L

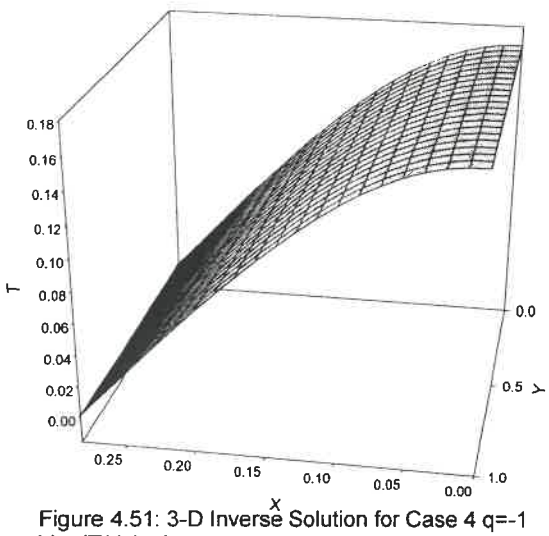

Figure 4.51: 3-D Inverse Solution for Case 4 q=-1 V=-dT/dx|x=L

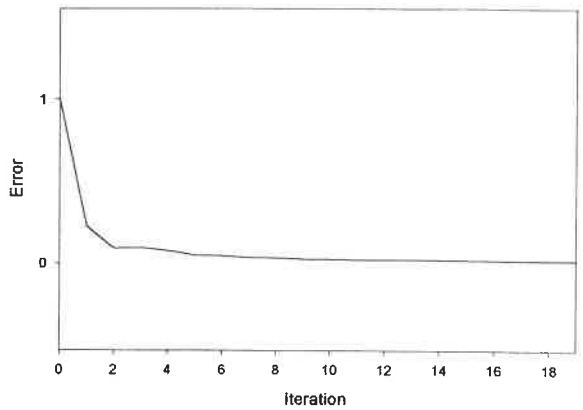

Figure 4.52: Error Evolution for Case 4 q=-1 V=-dT/dx|x=L

The general observations are that :

a. The recovered flux value is more similar to the actual value than that in Case $No.1$, The fluxes for the smaller noise level σ (0.001) is closer to the actual value than that for the higher noise level $\sigma = 0.04$.

b. The discrepancy between the temperature in the inverse solution and reality is less than that in Case $No.1$.

(6) Case $No.5$

For this case (From Fig.4.53 to Fig.4.59), the boundary flux increases linearly with time and the velocity is proportional to the temperature gradient as in the previous case.

$$q = q(t) = -t$$

$$V = -\frac{dT}{dx}\Big|_{x=1}$$

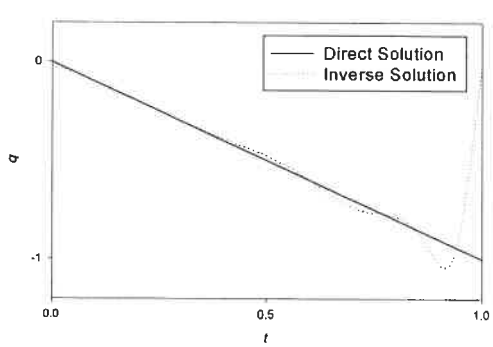

Figure 4.53: Heat Flux Vs Time for Case 5 q=-t,V=-dT/dx|x=L

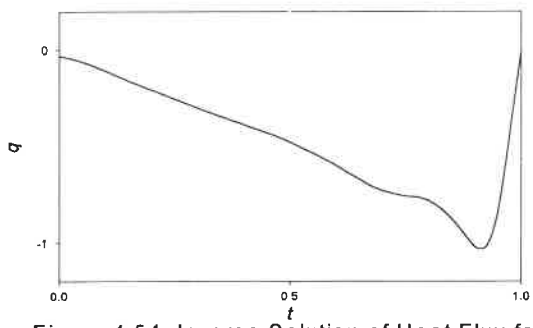

Figure 4.54: Inverse Solution of Heat Flux for Case 5 q=-t,V=-dT/dx|x=L, Sigma=0.001

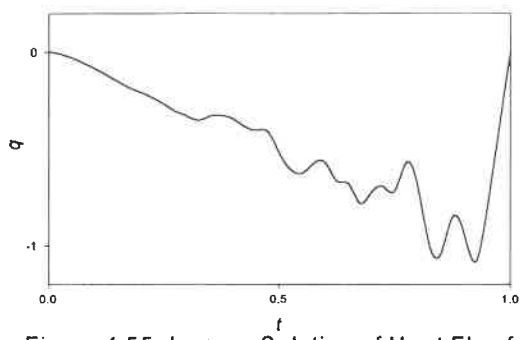

Figure 4.55: Inverse Solution of Heat Flux for Case 5 q=-t, V=-dT/dx|x=L, Sigma=0.04

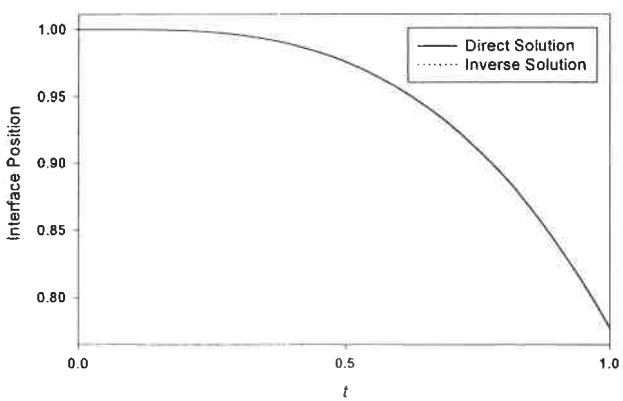

Figure 4.56 Interface Position Vs Time Case 5 q=-t V=-dT/dx|x=L

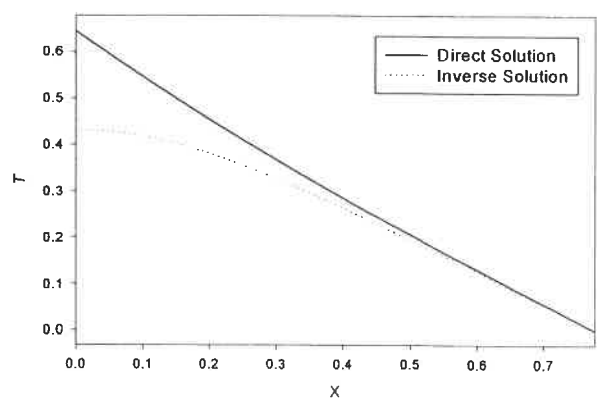

Figure 4.57 Contrast Between Direct Solution and Inverse Solution of Temperature for Case 5 q=-t, V=-dT/dx|x=L

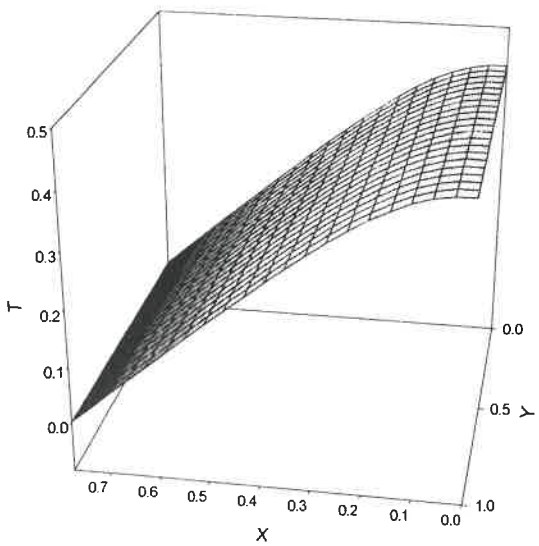

Figure 4.58: 3-D Inverse Solution for Case 5 q=-t V=-dT/dx|x=L

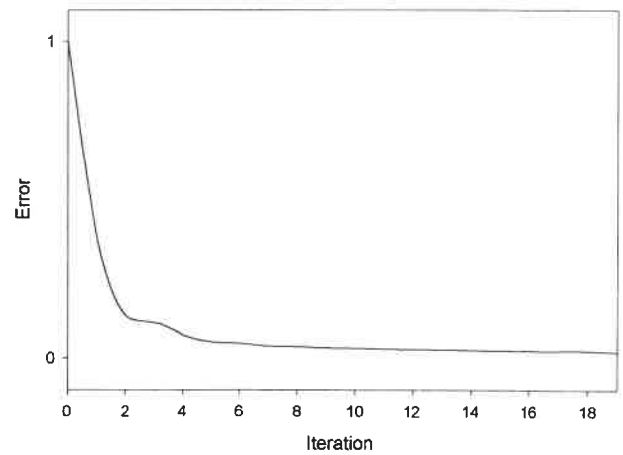

Figure 4.59: Error Evolution for Case 5 q=-t, V=-dT/dx|x=L

Comparison with Case No.2 reveals that the recovered value for flux, the inverse temperature, the error and the inverse flux (the noise is considered) is much closer to the real values. The discrepancy between the inverse solution and the actual solution for heat flux is also reduced.

(7) Case *No*.6 _ 1

For this case (From Fig.4.60 to Fig.4.66), the heat flux is oscillating $q = q(t) = -\sin(\omega\pi t)$ $(\omega = 1)$ and the velosity is given by

$$V = -\frac{dT}{dx}\Big|_{x=1}$$

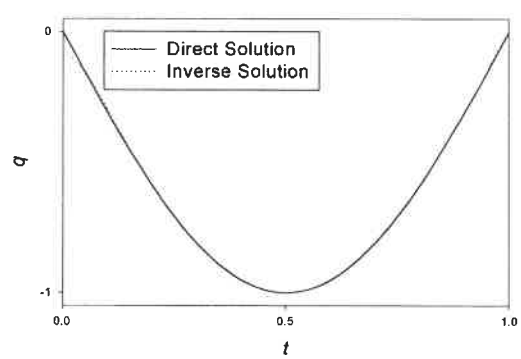

Figure 4.60: Heat Flux Vs Time for Case 6-1 q=-sin(w*PI*t),V=-dT/dx|x=L, w=1

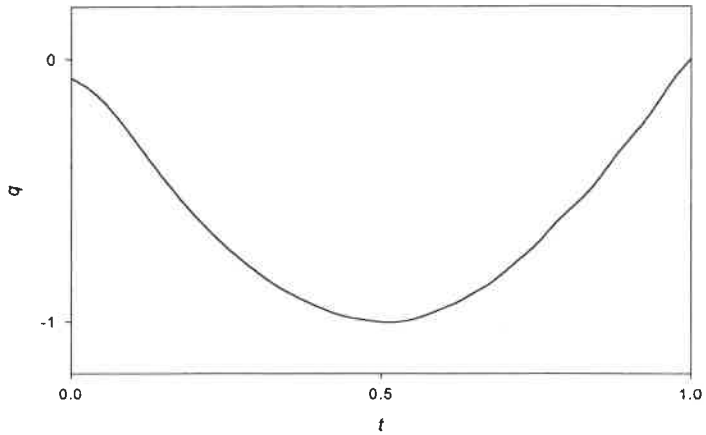

Figure 4.61: Inverse Solution of Heat Flux for
Case 6-1q=-sin(w*PI*t), V=-dT/dx|x=L, w=1, Sigma=0.001

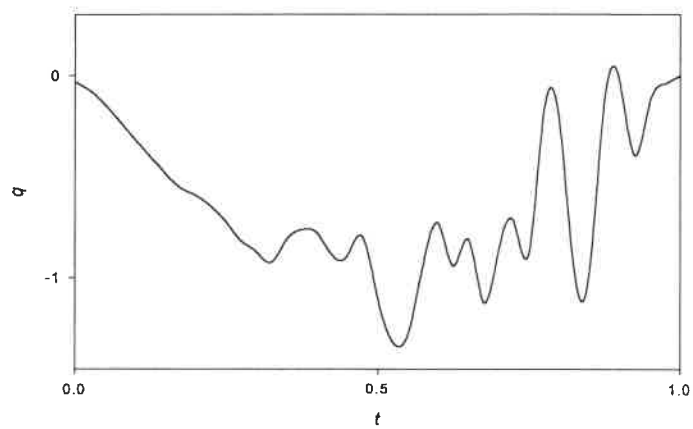

Figure 4.62: Inverse Solution of Heat Flux for
Case 6-1 q=-sin(w*PI*t), V=-dT/dx|x=L, w=1, Sigma=0.04

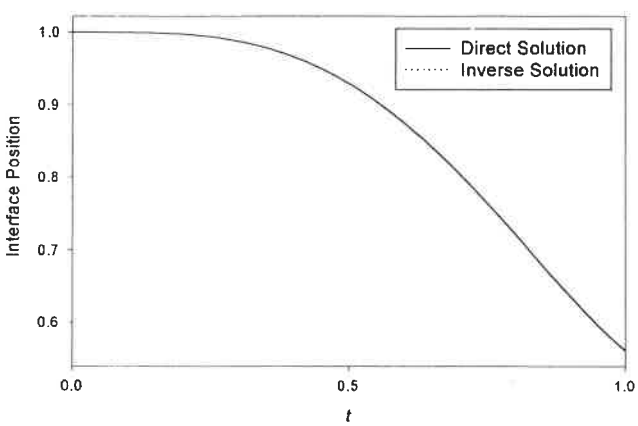

Figure 4.63: Interface Position Vs Time for Case 6-1
q=-sin(w*PI*t), V=-dT/dx|x=L, w=1

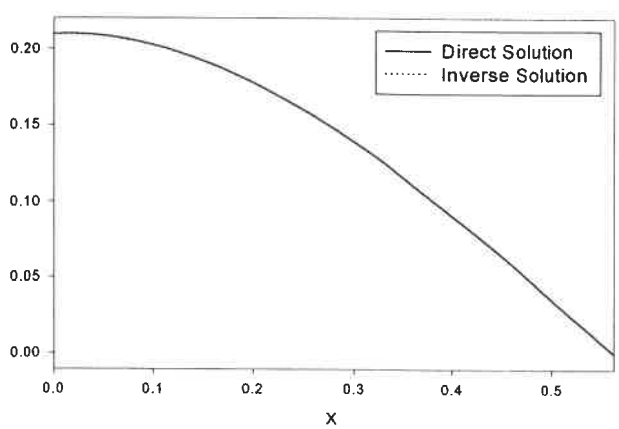

Figure 4.64: Contrast Between Direct Solution and Inverse
Solution of Temperature for Case 6-1 q=-sin(w*PI*t)
V=-dT/dx|x=L, w=1

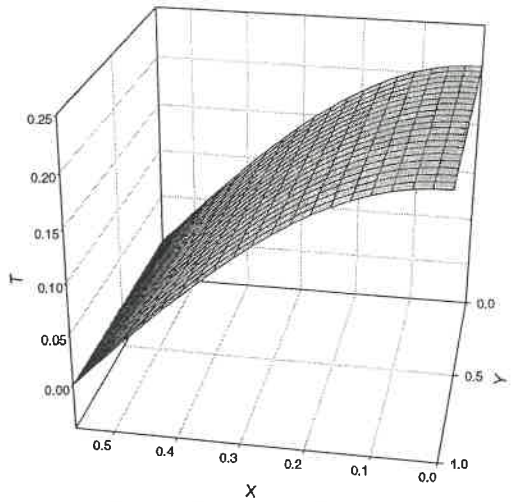

Figure 4.65: 3-D Inverse Solution for Case 6-1
q=-sin(w*PI*t), V=-dT/dx|x=L, w=1

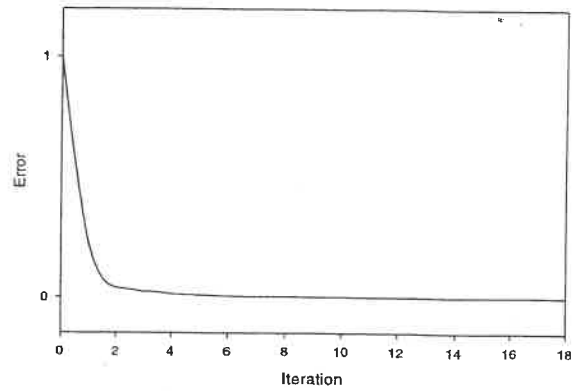

Figure 4.66: Error Evolution for Case 6-1 q=-sin(w*PI*t)
V=-dT/dx|x=L, w=1

The inverse flux solution is almost perfect.(Fig.4.60) The error(in Fig.4.66) is smaller than that in Case *No*.3_1. When the iteration number is greater than 2, the error becomes very small. From Fig.4.61 and Fig.4.62, the influence of noise on the recovered heat flux is shown.

(8) Case *No*.6_2

For this situation (From Fig.4.67 to Fig.4.71), $q = q(t) = -\sin(\omega\pi t)$ $(\omega = 10)$ and

$$V = -\frac{dT}{dx}\Big|_{x=1}$$

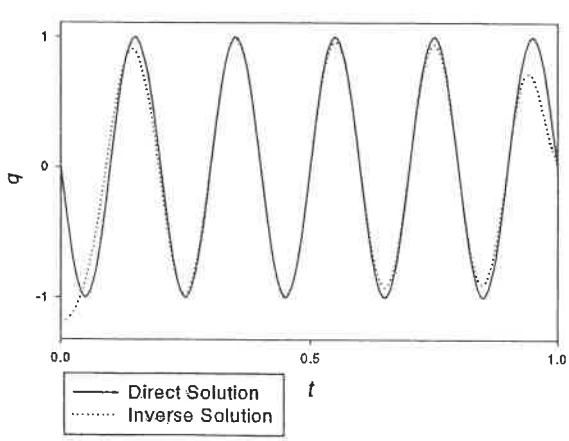

Figure 4.67: Heat Flux Vs Time for Case 6-2
q=-sin(w*PI*t),V=-dT/dx|x=L, w=10

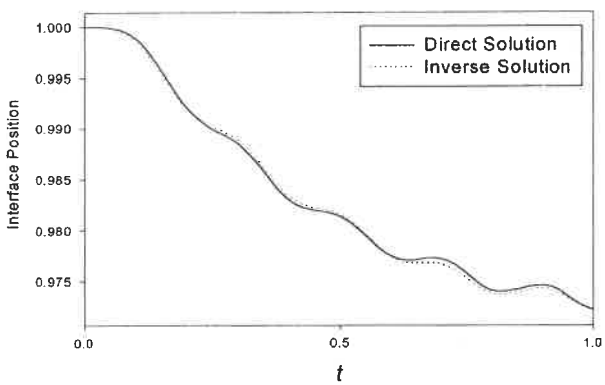

Figure 4.68: Interface Position Vs Time for Case 6-2
q=-sin(w*PI*t), V=-dT/dx|x=L, w=10

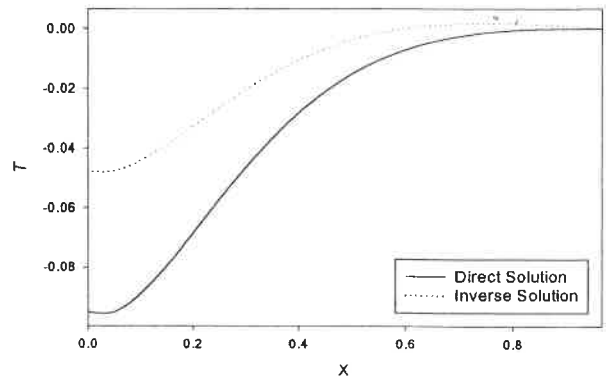

Figure 4.69: Contrast Between Direct Solution and Inverse Solution of Temperature for Case 6-2
q=-sin(w*PI*t), V=-dT/dx|x=L, w=10

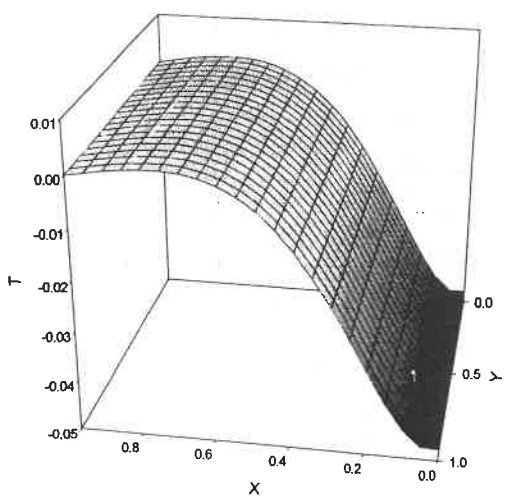

Figure 4.70: 3-D Inverse Solution for Case 6-2
q=-sin(w*PI*t), V=-dT/dx|x=L, w=10

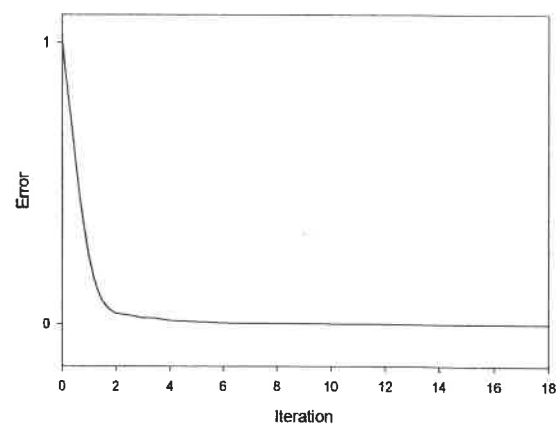

Figure 4.71: Error Evolution for Case 6-2
q=-sin(w*PI*t), V=-dT/dx|x=L, w=10

The inverse flux is recovered and shown in Fig.4.67. The discrepancy in the present case is smaller than that in Case $No.3_2$ and the number of iterations required is just 19. There is no need to go to 40,100 or more to get satisfactory results. The discrepancy between the inverse and direct temperatures and the error for the inverse solution is also less than that in Case $No.3_2$.

(9) Case $No.7$

For this situation (From Fig.4.72 to Fig.4.78), a constant flux $q = q(t) = -1.0$ is prescribed. The velocity of the boundary is imposed as time-varying, according to

$$V = \sin(\omega t)$$

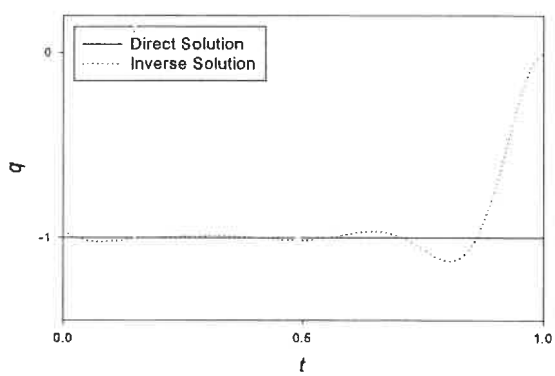

Figure 4.72: Heat Flux Vs Time for Case 7 q=-1 V=sin(wt), w=1

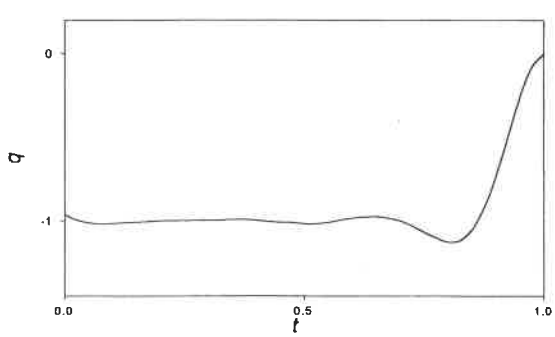

Figure 4.73: Inverse Solution of Heat Flux for Case 7 q=-1, V=sin(wt), w=1, Sigma=0.001

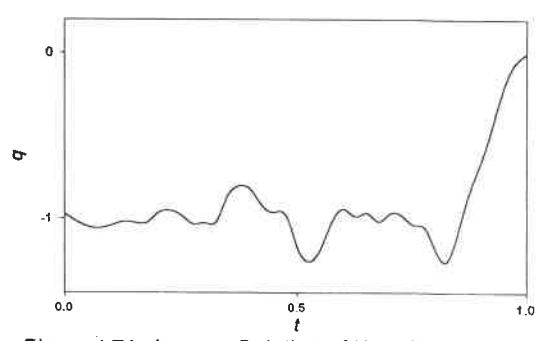

Figure 4.74: Inverse Solution of Heat Flux for Case 7 q=-1, V=sin(wt), w=1, Sigma=0.04

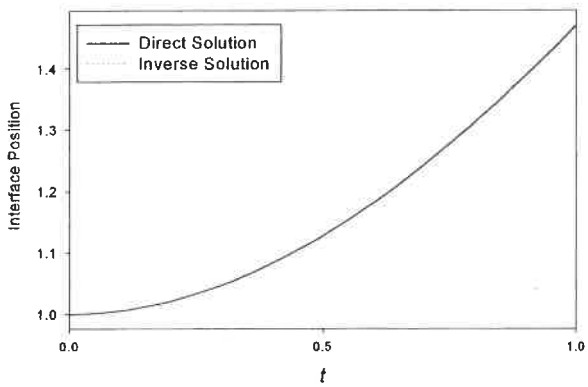

Figure 4.75: Interface Position Vs Time for Case 7 q=-1, V=sin(wt), w=1

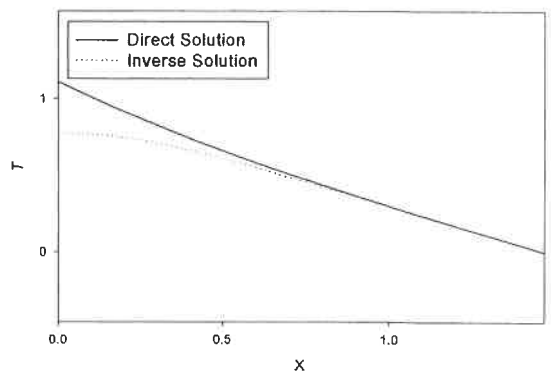

Figure 4.76: Contrast Between Direct Solution and Inverse Solution of Temperature for Case 7 q=-1 V=sin(wt), w=1

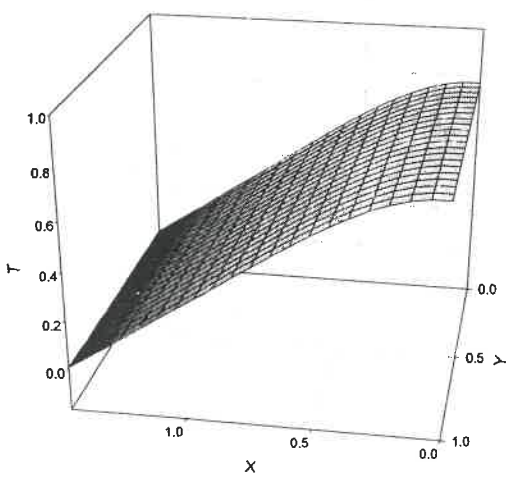

Figure 4.77: 3-D Inverse Solution for Case 7 q=-1 V=sin(wt), w=1

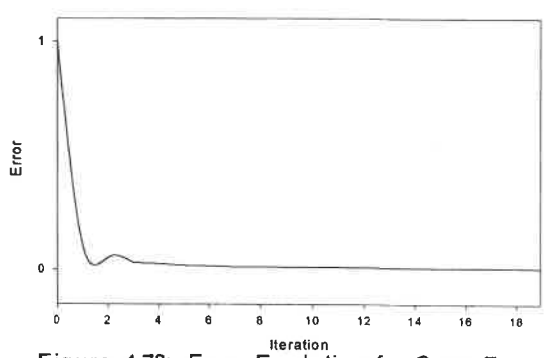

Figure 4.78: Error Evolution for Case 7 q=-1 V=sin(wt), w=1

The conclusion this time is that the discrepancies between the inverse and direct problem solution for heat flux and temperature are smaller than in Case *No*.1. The inverse heat flux (the effect of noise is considered) are shown in Fig.4.73 and Fig.4.74. The smaller σ level appears to cause smaller influence on the inverse heat flux.

(10) Case *No*.8

For this situation (From Fig.4.79 to Fig.4.85), $q = q(t) = -t$ (linear flux) with

$$V = \sin(\omega t)$$

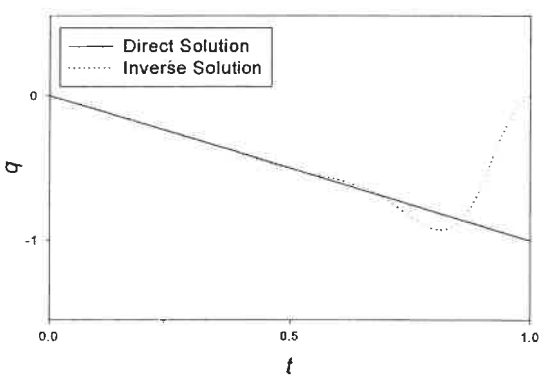

Figure 4.79: Heat Flux Vs Time for Case 8 q=-t V=sin(wt), w=1

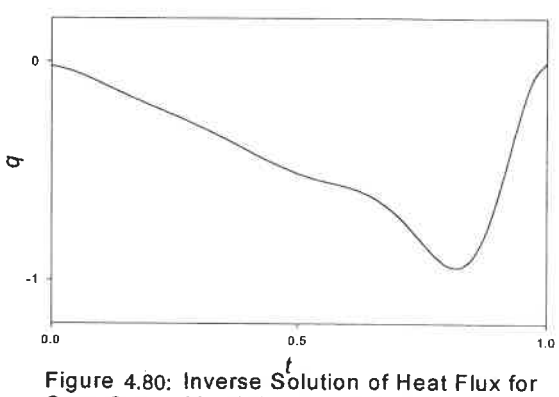

Figure 4.80: Inverse Solution of Heat Flux for Case 8 q=-t, V=-sin(wt), w=1, Sigma=0.001

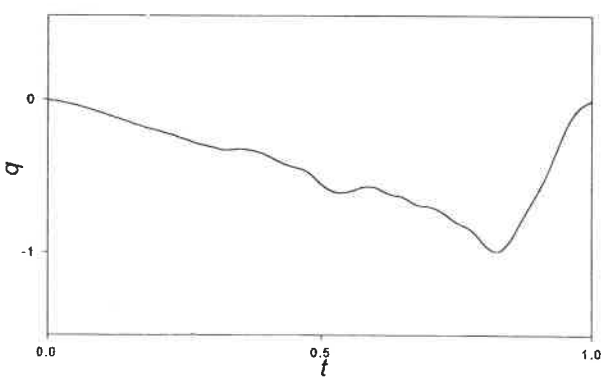

Figure 4.81: Inverse Solution of Heat Flux for Case 8 q=-t, V=sin(wt), w=1, Sigma=0.04

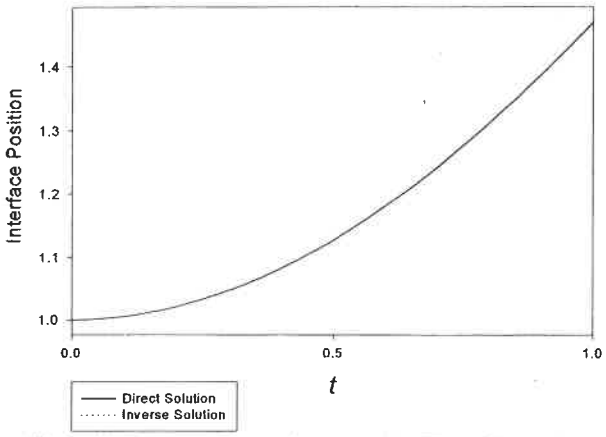

Figure 4.82: Interface Position Vs Time Case 8 q=-t V=sin(wt), w=1

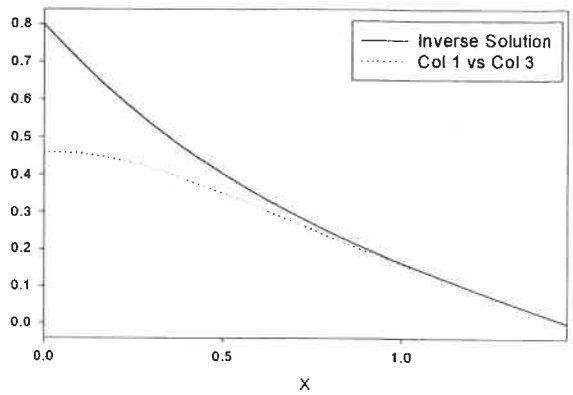

Figure 4.83: Contrast Between Direct Solution and Inverse Solution of Temperature for Case 8 q=-t V=sin(wt), w=1

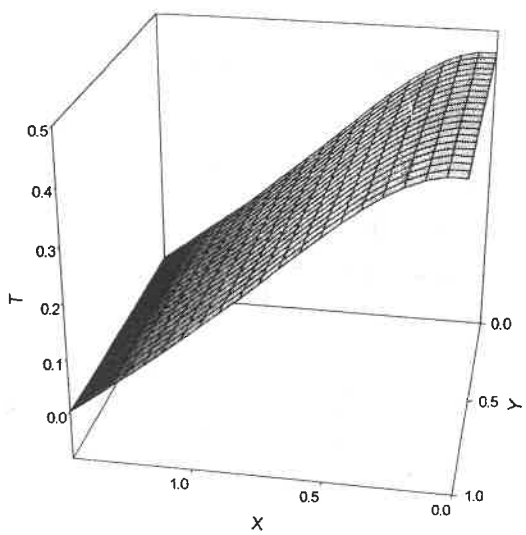

Figure 4.84: 3-D Inverse Solution for Case 8 q=-t, V=sin(wt), w=1

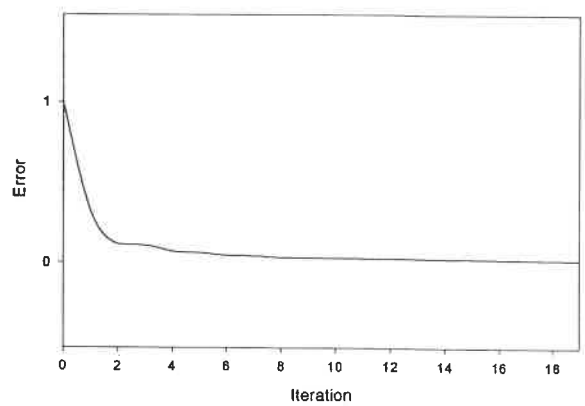

Figure 4.85: Error Evolution for Case 8 q=-t V=sin(wt), w=1

The various solutions for the inverse heat flux (shown in Fig.4.79), temperature(shown in Fig.4.83) and error(shown in Fig.4.85) are similar to Case No.#2, but the corresponding discrepancy level is much smaller, for noisy as well as for non-noisy temperature data.

(11) Case $No.9_1$

For this case (From Fig.4.86 to Fig.4.92), $q = q(t) = -\sin(\omega\pi t)$ $(\omega = 1)$ and $V = \sin(\omega t)$. Both q and V are sinusoidal functions of time.

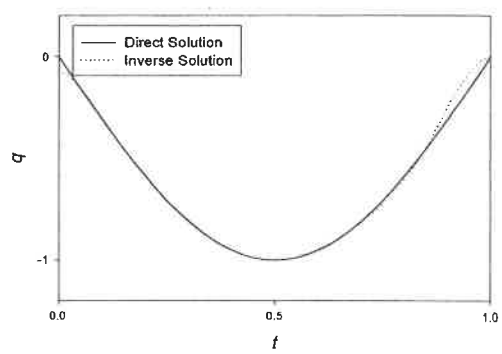

Figure 4.86: Heat Flux Vs Time for Case 9-1
q=-sin(w*PI*t), V=sin(wt), w=1

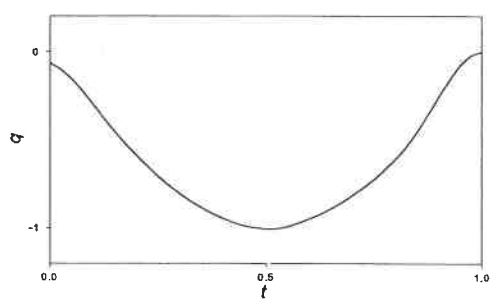

Figure 4.87: Inverse Solution of Heat Flux for Case 9-1 q=-sin(w*PI*t), V=sin(wt), w=1
Sigma=0.001

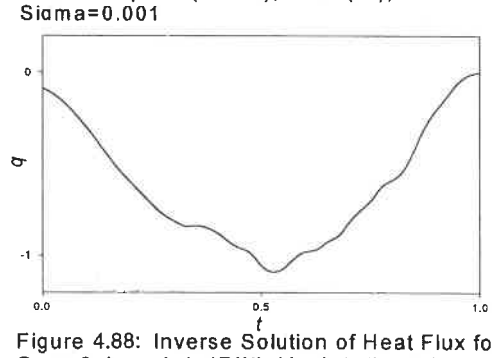

Figure 4.88: Inverse Solution of Heat Flux for Case 9-1q=-sin(w*PI*t), V=sin(wt), w=1
Sigma=0.04

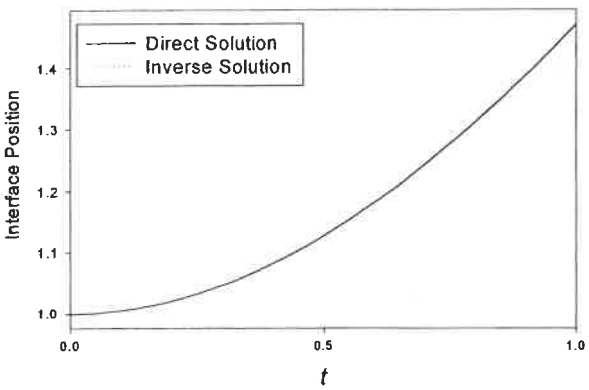

Figure 4.89: Interface Position Vs Time Case 9-1
q=-sin(w*PI*t), V=sin(wt), w=1

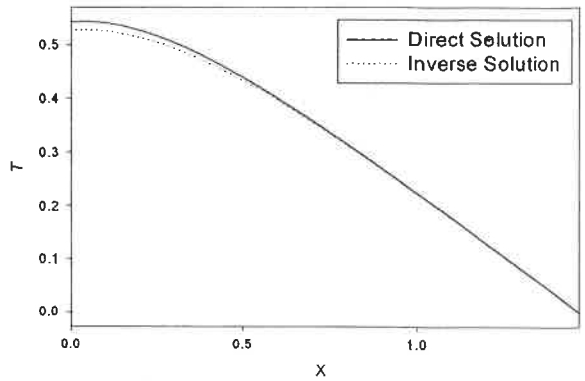

Figure 4.90: Contrast Between Direct Solution and Inverse Solution of Temperature for Case 9-1
q=-sin(w*PI*t), V=sin(wt), w=1

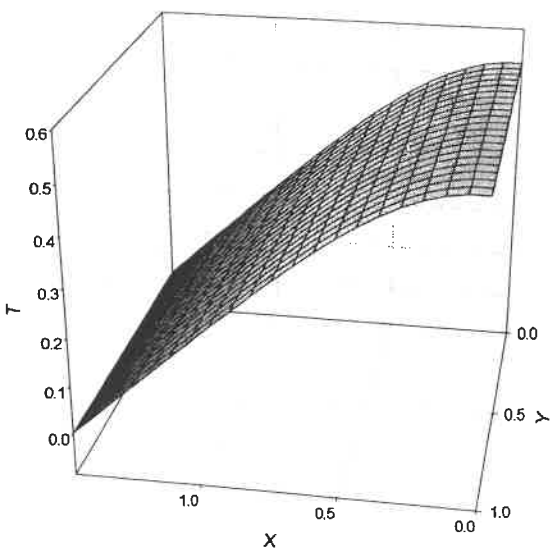

Figure 4.91: 3-D Inverse Solution Case 9-1
q=-sin(w*PI*t), V=sin(wt), w=1

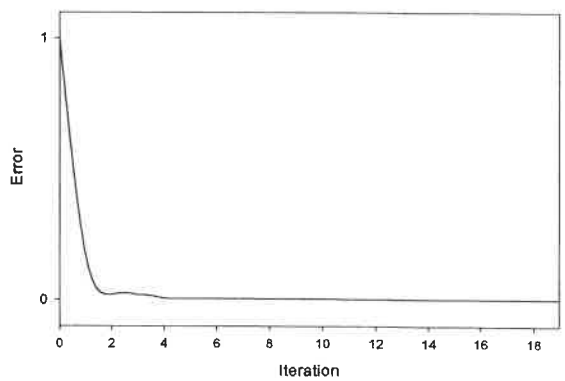

Figure 4.92: Error Evolution for Case 9-1
q=-sin(w*PI*t), V=sin(wt), w=1

The inverse solution procedure works very well. The recovered heat flux is very close to the actual value (shown in Fig.4.86) and the temperature is also close to the real value.

(12) Case *No*.9_2

For this case (From Fig.4.93 to Fig.4.99), we once more consider oscillating flux and velocity, but the frequency is different. We take: $q = q(t) = -\sin(\omega_1 \pi t)$ $(\omega_1 = 10)$ and $V = \sin(\omega_2 t)$ $(\omega_2 = 1)$

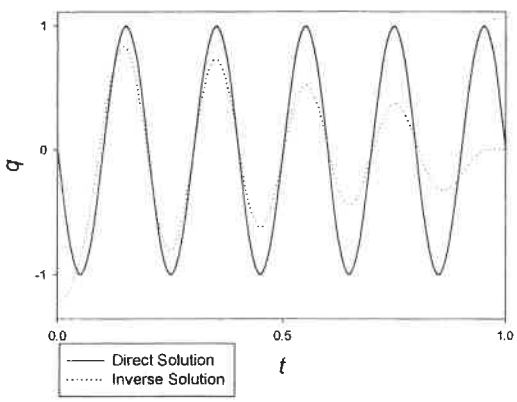

Figure 4.93: Heat Flux Vs Time for Case 9-2 q=-sin(w_1*PI*t),V=sin(w_2t), w_1=10, w_2=1 Iteration=19

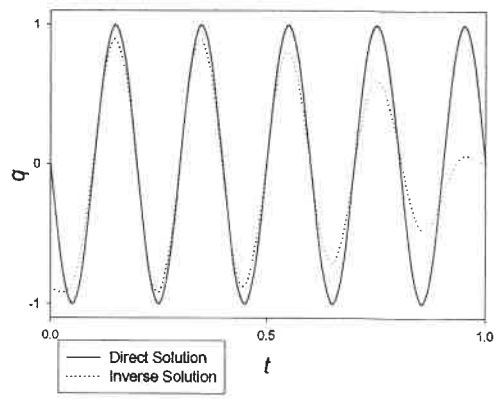

Figure 4.94:Inverse Solution of Heat Flux for Case 9-2 q=-sin(w_1*PI*t), V=sin(w_2t), w_1=10 w_2=1, Iteration=40

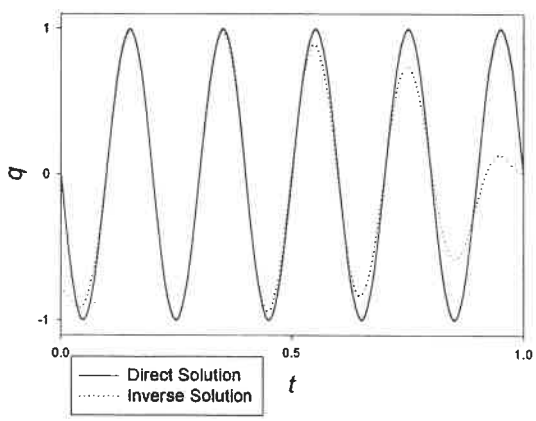

Figure 4.95:Inverse Solution of Heat Flux for Case 9-2 q=-sin(w_1*PI*t),V=sin(w_2t), w_1=10 w_2=1, Iteration=100

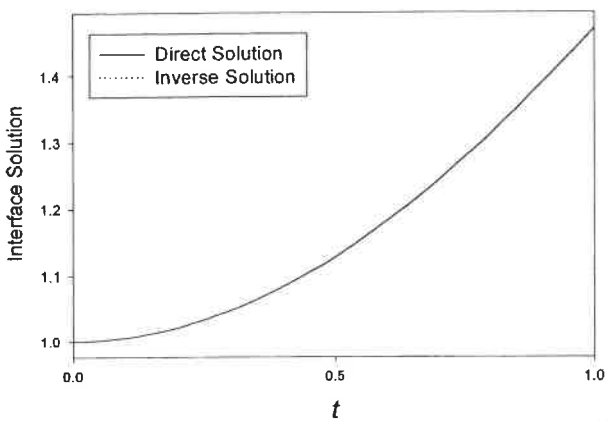

Figure 4.96: Interface Position Vs Time for Case 9-2
q=-sin(w1*PI*t),V=sin(w2t), w1=10, w2=1

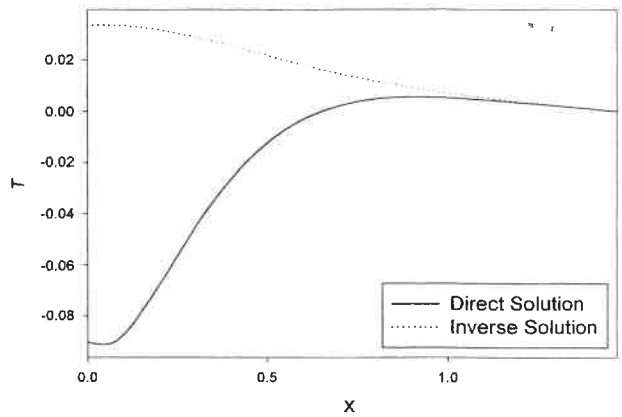

Figure 4.97: Contrast Between Direct Solution and Inverse Solution of Temperature for Case 9-2
q=-sin(w_1*PI*t), V=sin(w_2t), w_1=10, w_2=1

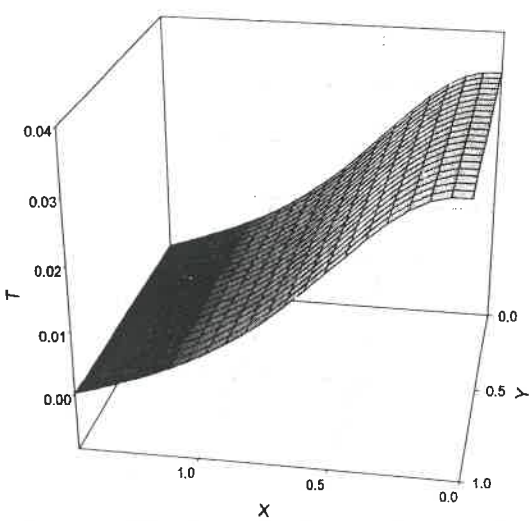

Figure 4.98: 3-D Inverse Solution for Case 9-2
q=-sin(w_1*PI*t), V=sin(w_2t), w_1=10, w_2=1

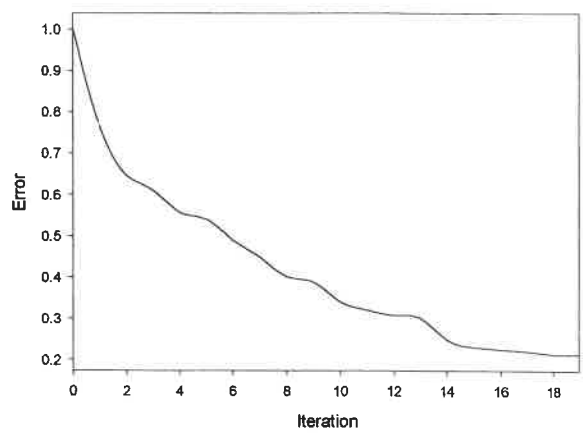

Figure 4.99: Error Evolution for Case 9-2
q=-sin(w_1*PI*t), V=sin(w_2t), w_1=10, w_2=1

For this kind of high frequency heat flux, we need much more iterations to get satisfactory results. We can see these results in Fig.4.93, Fig.4.94 and Fig.4.95. The smaller discrepancy is found after a great deal of iterations. According to the Fig.4.99, we can see that it is impossible to get the good results at the smaller iteration numbers because the error is very big.

Considering the Case *No*.3_1, Case *No*.3_2, Case *No*.6_1, Case *No*.6_2, Case *No*.9_1 and Case *No*.9_2, it is expected that there may be an optimal number of iterations leading to a reasonably accurate prediction of the unknown flux, before the high frequency noise components are recovered and start to adversely affect the solution. Experimentation with the number of iteration shows that a better solution is obtained after three or four iterations, approximately.

From Case *No*.1 to Case *No*.9_2 (total 12 cases), the 3_D graphs of temperature ~ (X, Y) are provided, because it is easier to get a global representation of the temperature field in a 3-D space graph.

The experimentations above show that the loss of accuracy and stability of the inverse solution is essentially due to the loss of sensitivity of temperature at the sensor's positions at high frequency. In fact, the samples mentioned above express that the accuracy and stability of the inverse solution actually depend on frequency, sensor position and the type of boundary condition.

To overcome the difficulty associated with high sensitivity, we should discuss the possibility of improvement on the optimal method and numerical discretization.

The level of agreement between the predictions and the exact solution is a good description of efficiency of the inverse problem solution method.

CONCLUSION

This project summarizes our research on the inverse problem of conduction with a moving boundary.

It concisely states the basic equations and basic steps for solving this kind of problem by the adjoint equation approach in conjunction with the conjugate gradient method.

By solving a series of direct problems in different situations, the benchmark solutions for the IHCP with a moving boundary have been found and the preliminary results have been obtained.

When solving an inverse conduction problem, it turns out very effective to approach the inverse conduction problem as an optimization problem.

This approach consists of establishing a set of three equations, namely, the direct equation, the sensitivity equation and adjoint equation. The method of solving an inverse conduction problem by a system of adjoint equations is very efficient in finding a boundary heat flux, for the design objective of obtaining a specified temperature distribution within the domain. On the basis of this method, the iteration process may be carried out automatically until the design criterion ($E < \delta$) is satisfied[4].

For the direct problem, this thesis considers 12 cases for numerical simulation. From Fig.4.1 to Fig.4.17, the temperatures and isotherm curves have been provided. The results shown in the Figures are reasonable.

For the inverse problem, we study 12 situations. The results obtained allow us to draw the conclusions below:

(1) This method can solve the inverse conduction problem and the results are reasonable and correct.

(2) In the graphs for heat flux as a function of time (from Case $No.1$ to Case $No.9_2$), the discrepancy between the actual and inverse value becomes larger with increasing time. There are two reasons for these phenomena.

a. it is caused by the cumulative effect of errors.

b. If the flux $(q) \neq 0$ when $t_f = 1.0$, it is cause of the main part of the discrepancy. For example, this can be seen in Fig.4.18, Fig.4.25 and so on. At each iteration step, the new flux estimate is proportional to adjoint temperature at $t = 1.0$. But in the cases discussed here, the adjoint temperature is Zero at $t_f = 1.0$. If the flux $(q) = 0$ at $t_f = 1.0$, the discrepancy for the flux is naturally much smaller, see for examples Fig.4.32 and so on.

(3) There is a jump in the solution for q when time is approaching the final value $t_f = 1.0$ if the flux $(q) \neq 0$ at $t_f = 1.0$, for the reason mentioned above that the adjoint temperature is Zero when time $=1.0(t_f)$

(4) In the Case $No.3_2$ and $No.9_2$, we can find that the results are better if the number of iterations is increased according to Fig.4.39, Fig.4.40, Fig.4.41, Fig.4.93, Fig.4.94 and Fig.4.95. And according to the curve of error versus time, the error is becoming smaller with increasing iterations.

(5) From Case $No.3_1$, Case $No.3_2$, Case $No.6_1$, Case $No.6_2$, Case $No.9_1$ and Case $No.9_2$, the algorithm has the ability to predict the various frequency components of a completely unknown heat flux in sequence, the lower frequency being recovered first. If the inverse problem includes high frequency, extra iterations are needed to get satisfactory results. Because the speed of convergence is frequency-dependent.

(6) For each case, the noise with the average value $=0$ is considered. It has large influence on the inverse heat flux. It is shown in Fig.4.19, Fig.4.20 and so on. In the cases discussed in this thesis, $\sigma = 0.001$ always provides better solution than $\sigma = 0.04$ For example, Fig.4.19 and Fig.4.20 clearly show the phenomenon.

In a word, this thesis briefly introduces the basic method and ideas for solving the inverse problem of conduction.

As what is stated above, the precision and convergence are largely determined by boundary conditions and the way of dividing grids and some parameters. Hence, for solving IHCP more effectively, we expect to be able to do some improvement on discretization formula and optimal method so as to avoid the complexity of high sensitivity of IHCP to noise and obtain satisfactory convergent results with good stability. That is also left for the future work.

REFERENCES

[1] BECK, J. V., BLACKWELL B. and St – Clair, C. R. JR. (1985). Inverse Heat Conduction: Ill – posed Problems, Wiley, New York.

[2] ALIFANOV O.M. (1994). Inverse Heat Transfer Problems. Springer-Verlag, New York.

[3] ALIFANOV O.M., ARTYUKHIN E.A., and RUMYANTSEV S.V. (1996). Extreme Methods for Solving Ill-Posed Problems with Applications to Inverse Heat Transfer Problems. Begell House, New York.

[4] ALIFANOV O.M. and KEROV N.V. (1981). Determination of external thermal load parameters by solving the two-dimensional inverse heat conduction problem. Journal of Engineering Physics, 41(4):1049-1053.

[5] HUANG C.H. and OZISIK M.N. (1991). Direct integration approach for simultaneously estimating temperature dependent thermal conductivity and heat capacity. Numerical Heat Transfer, Part A, 20:95-100.

[6] KRAVARIS C. and SEINFELD J.H. (1985). Identification of parameter system by regularization. SIAM J. Contr. Optimization, 23:217-241.

[7] MEJIA C.E. and MURIO D.A. (12.1995). Numerical identification of diffusivity coefficient and initial condition by discrete mollification. Computers Math.Applic., 30:35-50.

[8] ZABARAS N., RUAN Y., and RICHMOND O. (1992). On the design of two dimensional Stefan processes with desired freezing front motions. Numer. Heat

Transfer, 21B: 307- 325.

[9] ZABARAS N. (1990). Inverse finite element techniques for the analysis of solidification processes. Int. j. numer. Methods engr., 29: 1569-1587.

[10] ZABARAS N. and KANG S. (1994). On the solution of an ill-posed inverse design solidification problem using minimization techniques in finite and infinite dimensional spaces. Int. j. numer. Methods engr., 36: 3973-3990.

[11] KANG S. and ZABARAS N. (1995). Control of the freezing interface motion in two-dimensional solidification processes using the adjoint method. Int. j. numer. Methods engr., 38: 63 - 80.

[12] ZABARAS N. and NGUYEN T. HUNG (1995). Control of the freezing interface morphology in solidification processes in the presence of natural convection. Int. j. numer. Methods engr., 38: 1555 - 1578.

[13] CANNON J.R. and HILL C.D. (1967). Existence, uniqueness, stability, and monotone dendence in a Stefan problem for the heat equation. J. Math. Mech., 17:1 - 19.

[14] COLTON D. L. and REEMTSEN R. (1984). The numerical solution of the inverse Stefan problem in two space variables. SIAM J. Appl. Math., 44: 996 -1013, 1984.

[15] CHEN J. (1998). Inverse Heat Conduction Problem in a Cavity. M. Sc.. A. thesis Mechanical Engineering, École Polytechnique de Montréal.

[16] STOLZ, G., Jr. (1960). Numerical Solutions to an Inverse Problem of Heat Conduction for Simple Shapes, J.Heat Transfer 82, 20- 26.

[17] MIRSEPASSI, T. J. (1959). Heat - Transfer Charts for Time - Variable Boundary Conditions, Br. Chem. Eng. 4, 130 - 136.

[18] MIRSEPASSI, T. J. (1959). Graphical Evaluation of Convolution Integral, Mathematical Tables and Other Aides to Computation 13, 202 - 212.

[19] SHUMAKOV, N. V. (1957). A Method for the Experimental Study of the Process of Heating a Solid Body, Soviet Physics - Technical Physics (Translated by American Institute of Physics) 2, 771.

[20] BECK, J. V. (1961 30-Mar.). Correction of Transient Thermocouple Temperature Measurements in Heat - Conducting Solids, Part II, the Calculation of Transient Heat Fluxes Using the Inverse Convolution, AVCO Corp., Res. And Adv. Dev. Div., Wilmington, MA., Tech. Report RAD - TR -7-60-38 (Part II).

[21] BECK, J. V. (1962). Calculation of Surface Heat Flux from an Internal Temperature History, ASME Paper, 62-HT-46.

[22] BECK, J. V. (1968). Surface Heat Flux Determination Using an Internal Method, Nucl. Eng. Des. 7, 170-178.

[23] BECK, J. V., and Wolf, H. (1965). The Nonlinear Inverse Heat Conduction Problem, ASME Paper, 65-HT-40.

[24] BECK, J. V. (1970). Nonlinear Estimation Applied to the Nonlinear Heat Conduction Problem, Int. J. Heat Mass Transfer 13, 703-716.

[25] BECK, J. V. (1979). Criteria for Comparison of Methods of Solution of the Inverse

Heat Conduction Problem, Nucl. Eng. Des. 53, 11-22.

[26] BECK, J. V., Litkouhi, B., and St. Clair, C.R., Jr. (1982). Efficient Sequential Solution of the Nonlinear Inverse Heat Conduction Problem, Numer. Heat Transfer 5, 275-286.

[27] BLACKWELL, B.F. (1968). A New Iterative Technique for Solving the Implicit Finite - Difference Equations for the Inverse Problem of Heat Conduction, unpublished technical report, Sandia Laboratories, Albuquerque, NM.

[28] BLACKWELL, B.F. (1981). An Efficient Technique for the Numerical Solution of the One-Dimensional Inverse Problem of Heat Conduction, Numer. Heat Transfer 4, 229-239.

[29] MULHOLLAND, G. P., Gupta, B. P., and San Martin, R. L. (1975). Inverse Problem of Heat Conduction in Composite Media, ASME Paper, 75-WA/HT-83.

[30] MULHOLLAND, G. P. and San Martin, R. L. (1971). Inverse Problem of Heat Concuction in Composite Media, Third Canadian Congress of Applied Mechanics, Calgary, Alberta, Canada.

[31] MULHOLLAND, G. P., and Cobble, M. H. (1972). Diffusion through Composite Media, Int. J. Heat Mass Transfer 15, 147-152.

[32] MULHOLLAND, G. P. and San Martin, R. L. (1973). Indirect Thermal Sensing In Composite Media, Int. J. Heat Mass Transfer 16, 1056-1060.

[33] WILLIAMS, S. D. and CURRY, D. M. (1977). An Analytical Experimental Study for Surface Heat Flux Determination, J. Spacecraft 14, 632-637.

[34] BURGGRAF, O. R. (1964). An Exact Solution of the Inverse Problem in Heat Conduction Theory and Applications, J. Heat Transfer 86C, 373-382.

[35] IMBER, M. and KHAN, J. (1972). Prediction of Transient Temperature Distributions with Embedded Thermocouples, AIAA J. 10, 784-789.

[36] LANGFORD, D. (1967). New Analytic Solutions of the One-Dimensional Heat Equation for Temperature and Heat Flow Rate Both Prescribed at the Same Fixed Boundary (with Applications to the Phase Change Problem), Q. Appl. Math. 24, 315-322.

[37] TIKHONOV, A. N. and ARSENIN, V. Y. (1977). Solutions of Ill-Posed Problems, V. H. Winston & Sons, Washington, D.C..

[38] HILLS, R. G. and MULHOLLANDulholland, G. P. (1979). Accuracy and Resolving Power of One-Dimensional Transient Inverse Heat Conduction Theory as Applied to Discrete and Inaccurate Measurements, Int. J. Heat Mass Transfer 22, 1221-1229.

[39] BACKUS, G. and GILBERT, F. (1970) Uniqueness in the Inversion of Inaccurate Gross Earth Data, Phil. Trans. R. Soc. London Ser. A 266, 123-192.

[40] NOLET, G. (1978). Simultaneous Inversion of Seismic Data, Geophys. J. R. Astr. Soc. 55, 679-691.

[41] ZHANG X. and NGUYEN T. H. (1992). Numerical Study of Convection Heat Transfer during the Melting of Ice in a Porous Layer

[42] WOLFE M. A. (1978). Numerical Method Unconstrained Optimization

[43] JARNY Y., OZISIK M. N. and BARDON J. P. (1991). A general optimization method using adjoint equation for solving multidimensional inverse heat conduction, Int. J. Heat Mass Transfer 34 (11) 2911-2919

[44] MERIC R. A. (1985). Optimization of thermal conductivities of isotropic and orthotropic solids, J. Heat Transfer 107 508-513

[45] NGUYEN T. H. (1995). An optimization approach to some inverse convection problems, in: Proceedings of International Conference of Analysis and Mechanics of International Conference on Analysis and Mechanics of Continuous Media, Ho-Chi Minh City, pp. 188-195

[46] PRUD'HOMME M. and NGUYEN T. H. (1997). Whole time-domain approach to the inverse natural convection problem, Num. Heat Transfer 32 169-186 (Part A)

[47] PRUD'HOMME M. and NGUYEN T. H. (1999). Fourier analysis of conjugate gradient method applied to inverse heat conduction problems, International Journal of Heat and Mass Transfer 42 4447-4460

[48] PATANKAR, S. V. (1980). Numerical Heat Transfer and Fluid Flow, Mc Graw - Hill, New York.

[49] PRUD'HOMME M. and NGUYEN T. H. (1996). Methode de solution par volumes de contrôle du probleme inverse en convection naturalle. EPM/RT-96/10- École Polytechnique de Montréal.

ÉCOLE POLYTECHNIQUE DE MONTRÉAL
3 9334 00292764 6